168
10

To the Graduate Council:

I am submitting herewith a thesis written by Gary W. Selby entitled "The Absorption of Dilute Nitrogen Oxides into Aqueous Media Using a Structured Packing." I have examined the final copy of this thesis for form and content and recommend that it be accepted in partial fulfillment of the requirements for the degree of Master of Science, with a major in Chemical Engineering.

Robert M. Counce

Robert M. Counce,
Major Professor

We have read this thesis
and recommend its acceptance:

Joseph J. Perona

George C. Frazier

Accepted for the Council:

Lewis Winkel

Vice Provost
and Dean of The Graduate School

STATEMENT OF PERMISSION TO USE

In presenting this thesis in partial fulfillment of the requirements for a Master's degree at The University of Tennessee, Knoxville, I agree that the Library shall make it available to borrowers under rules of the Library. Brief quotations from this thesis are allowable without special permission, provided that accurate acknowledgment of the source is made.

Permission for extensive quotation from or reproduction of this thesis may be granted by my major professor, or in his absence, by the Head of Interlibrary Services when, in the opinion of either, the proposed use of the material is for scholarly purposes. Any copying or use of the material in this thesis for financial gain shall not be allowed without my written permission.

Signature Gary Selby

Date May 15, 1986

THE ABSORPTION OF DILUTE NITROGEN OXIDES INTO AQUEOUS MEDIA USING A STRUCTURED PACKING

A Thesis

Presented for the

Master of Science

Degree

The University of Tennessee, Knoxville

Gary W. Selby

June 1986

ACKNOWLEDGMENTS

The author would like to express his deepest appreciation for the guidance and patience given to him by his major professor, Dr. Robert M. Counce. Dr. Counce's advice and support have been invaluable to the completion of this thesis. He would also like to thank Dr. Joe Perona and Dr. George Frazier for agreeing to serve on his thesis committee.

Special thanks are given to Al Carter and Aileen Cagle for their help with experimental equipment. The author would like to recognize Anne Upchurch for her diligent work in typing this thesis. The encouragement and support of family and friends, especially my mother and father, is greatly appreciated.

ABSTRACT

Pilot-plant experiments on the aqueous scrubbing of dilute NO_x gas mixtures at atmospheric pressure have been conducted using an absorber filled with high efficiency packing. NO_x removal efficiencies of 10 to 70% were obtained for gas mixtures of 125 to 2500 ppm NO_x; the NO_x species were predominantly NO_2^* (NO_2 and N_2O_4). The 0.102-m-id absorber was packed with Koch Sulzer packing (Type BX) to a depth of 0.8 m.

The experimental results are in good agreement with a model based on the absorption/hydrolysis of N_2O_4 and NO_2. A liquid phase mass transfer coefficient of 4.982×10^{-4} m/s was calculated by data analysis. The value of this coefficient is reasonable compared to mass transfer coefficients of other packings. The gas-liquid interfacial area of the packing was determined to be 690. m^{-1}. This interfacial area was found to be independent of the liquid rate which is in agreement with other studies.

TABLE OF CONTENTS

LIST OF TABLES

LIST OF FIGURES

FIGURE PAGE

FIGURE PAGE

LIST OF SYMBOLS AND ABBREVIATIONS

a_i	gas-liquid interfacial area, m^{-1}
d	differential operator
D	diffusivity, m^2/s
e	natural exponential function
(g)	gas
G	gas rate, LPM
G'	gas flux, $kgmol/m^2$-s
H_i	Henry's Law constant for component i, m^3-atm/kgmol
HNO_x	$HNO_2 + HNO_3$
ID	inside diameter, m
k_i	reaction rate constant for equation i, s^{-1}
k_L	liquid phase mass transfer coefficient, m/s
K_i	equilibrium constant for equation i
(l)	liquid
log	base 10 logarithmic function
ln	base e logarithmic function
L	liquid rate, LPM
LPM	liters per minute
n_i	moles of component i, kgmol
N_i	absorption rate of component i, $kgmol/m^2$-s
NO_2^*	$NO_2 + N_2O_4$

NO_x	$NO_2^* + NO$
OD	outside diameter, m
ppm	parts per million
P	pressure, atm
P_i	partial pressure of component i, atm
P_T	total pressure, atm
r_i	rate of reaction for equation i, kgmol/s
R	gas law constant, m^3 - atm/kgmol - K
T	temperature, K
V	volume, m^3
X_i	fractional conversion of component i
Y_i	mole fraction of component i
z	differential column height, m
Z	total column height, m
α	fraction of N_2O_4 dissociated in gas phase

CHAPTER 1

INTRODUCTION

The absorption of nitrogen oxides into aqueous media is an important process in many industries, especially in the manufacture of nitric acid. More recently the increased public concern for air pollution control has greatly increased the need to understand the chemistry of nitrogen oxides absorption. Despite the tremendous amount of literature on this subject, a complete understanding of this process is not available.

Pilot-plant experiments on the aqueous scrubbing of dilute NO_x gas mixtures at atmospheric pressure have been conducted. The absorber was filled with high efficiency Koch/Sulzer packing (Type BX) to a depth of 0.80 m. Gas rate, liquid rate, and inlet NO_x concentration were varied to study the effect on removal efficiencies. NO_2^* removal efficiencies of 10 to 70% were obtained for inlet NO_x mixtures ranging from 125 to 2500 ppm. During these runs the predominant NO_x species were NO_2^* ($NO_2 + 2N_2O_4$).

The experimental results are in good agreement with a model based on the absorption/hydrolysis of N_2O_4 and NO_2. The gas-liquid interfacial area was determined to be approximately 690. m^{-1}. A value of 4.982×10^{-4} m/sec

was also determined for the liquid-phase mass transfer coefficient. The interfacial remained relatively constant over the range of conditions studied, which is in agreement with Koch/Sulzer publications.

CHAPTER 2

LITERATURE REVIEW

The scrubbing of nitrogen oxides is an important industrial process. Nitrogen oxides arise from the production of nitric acid, metal plating and finishing operations, and in the processing of nuclear fuels. Knowledge of the mechanisms involved in NO_x absorption are becoming more important to these industries. The increased air pollution problems associated with nitrogen oxides further underscore the need for a better understanding of the NO_x system.

This understanding of the NO_x system was greatly enhanced by the development of the theory of combined absorption and chemical reaction (Danckwerts, 1970). This theory is currently used in NO_x scrubber design and to interpret laboratory scale absorption data (Sherwood, Pigford, and Wilke, 1975; Hoftyzer and Kwanten, 1972; Counce, 1979).

This literature review begins with the presentation of important species and reactions in the NO_x-HNO_x-H_2O system. This portion of the review is based on the extensive review by Counce (1979). Characteristics of the packing material (Koch/Sulzer Type BX) are then considered, followed by a review of some current

literature concerning the absorption of low NO_x concentrations and a literature summary.

The NO_x--HNO_x--H_2O System

The important species in the NO_x--HNO_x--H_2O chemical system are NO, NO_2, N_2O_3, N_2O_4, HNO_2, HNO_3, and H_2O. Attention will first be directed toward the gas-phase reactions. The solubilities of the NO_x species will then be compared, followed by the liquid-phase reactions which contribute to the NO_2 absorptive flux from the gas to the liquid phase.

Gas phase reactions. The important NO_x reactions to consider in the gas-phase are:

$$2NO_2 \overset{K_1}{\rightleftharpoons} N_2O_4 \qquad (2\text{-}1)$$

$$NO + NO_2 \overset{K_2}{\rightleftharpoons} N_2O_3 \qquad (2\text{-}2)$$

$$NO + NO_2 + H_2O \overset{K_3}{\rightleftharpoons} 2HNO_2 \qquad (2\text{-}3)$$

$$3NO_2 + H_2O \overset{K_4}{\rightleftharpoons} 2HNO_3 + NO \qquad (2\text{-}4)$$

$$2NO + O_2 \xrightarrow{k_5} 2NO_2 \qquad (2\text{-}5)$$

The partial pressures of "chemical NO_2" (NO_2^*) and NO_x are defined in terms of the other nitrogen oxide species:

$$P_{NO_2}^* = P_{NO_2} + 2P_{N_2O_4} \tag{2-6}$$

$$P_{NO_x} = P_{NO_2}^* + P_{NO} \tag{2-7}$$

Verhoek and Daniels (1931) gave the following correlation for the equilibrium constant for Equation (2-1):

$$\log K_1 = 9.8698 - \left(\frac{3.98}{T(K)}\right) \tag{2-8}$$

The equilibrium constant K_1 is also correlated by Hoftyzer and Kwanten (1972) and by Bronsted (1922) in Equations (2-9) and (2-10), respectively.

$$K_1 = (0.707 \times 10^{-9}) \exp\left(\frac{6866.}{T(K)}\right) \tag{2-9}$$

$$\log K_1 = \left(\frac{2993.}{T(K)}\right) - 9.226 \tag{2-10}$$

In this work, the correlation of Bronsted (1922) was used. Beattie and Bell (1957) calculated values for the equilibrium constant of Equation (2-2) at low N_2O_3 partial pressures and covered a temperature range of 278-318 K. Their work was expressed by Hoftyzer and Kwanten (1972) as:

$$K_2 = (66.15 \times 10^{-9}) \exp\left(\frac{4740.}{T(K)}\right) \qquad (2\text{-}11)$$

Table 2-1 displays values of the equilibrium constant for Equation (2-3) as observed by various researchers. Hoftyzer and Kwanten (1972) gave the correlation for K_3 in Equation (2-12):

$$K_3 = (0.187 \times 10^{6}) \exp\left(\frac{4723.}{T(K)}\right) \qquad (2\text{-}12)$$

The thermodynamics of Equation (2-4) had caused much confusion (Wendell and Pigford, 1958) among researchers. But if a two-phase system is considered,

$$3NO_2(g) + H_2O_{(g)} \overset{K_4'}{\rightleftharpoons} 2HNO_3(l) + NO_{(g)} \qquad (2\text{-}13)$$

the reaction is favored thermodynamicly (Forsythe and Giaugue, 1942). The second phase is often seen as a mist or fog and occurs when the partial pressure of HNO_3 exceeds about 50 ppm at ambient conditions (Goyer, 1963) or if it exceeds its vapor pressure.

The gas-phase reaction of NO_2 and H_2O was studied by England and Corcoran (1974). The reaction of NO and HNO_3 was studied by Smith (1947) and by Lefers et al. (1980). Values of rate constants were calculated in these studies, which compare favorably with theoretical calculations.

Table 2-1. Equilibrium Constants for the Gas Phase Reaction of NO, NO_2, HNO_2, and H_2O.

Temperature (K)	Values of K_3 (atm^{-2}) Obtained by Various Researchers			
	Wayne and Yost	Ashmore and Tyler	Karavaev and Skvortsov	Waldorf and Babb
293		1.56		
298	1.74		1.60	2.38
313		0.641		
325			0.445	
333		0.250		
350			0.156	
353		0.112		
375			0.609×10^{-1}	
400			0.267×10^{-1}	
425			0.132×10^{-1}	
450			0.704×10^{-2}	
475			0.398×10^{-2}	
500			0.236×10^{-2}	

Sources:

1. L. G. Wayne and D. M. Yost, J. Chem. Phys. 19: 41 (1951).

2. G. Ashmore and B. J. Tyler, J. Chem. Soc. 1017 (1961).

3. M. Karavaev and G. A. Skvortsov, Russ. J. Phys. Chem. 36: 566 (1962).

4. D. M. Waldorf and A. L. Babb, J. Chem. Phys. 39: 432 (1963).

More recently reaction (2-4) was investigated by McKinnon, Mathieson, and Wilson (1979). They report a rate constant of 8.4 m^3/kgmol-s for the reaction of nitric oxide and nitric acid at 298 K. They also conclude that the reaction is homogeneous and that nitrous acid is an intermediate specie.

A summary of reaction rate constants for Equation (2-5) are given in Table 2-2. All researchers confirmed third-order kinetics, which is consistent with the following rate equation:

$$r_5 = k_5 P_{NO}^2 P_{O_2} \qquad (2\text{-}14)$$

Solubilities of NO_x and HNO_x species in water. The solubilities of the NO_x and HNO_x species are exhibited in Table 2-3. The range of these Henry's Law constants, from very soluble to very insoluble, point out the individual roles that these species play in the design of aqueous NO_x absorption processes. These equilibrium equations rank the species from least to most soluble:

$$NO_{(g)} \rightleftharpoons NO_{(l)} \qquad (2\text{-}15)$$

$$NO_{2(g)} \rightleftharpoons NO_{2(l)} \qquad (2\text{-}16)$$

$$N_2O_{3(g)} \rightleftharpoons N_2O_{3(l)} \qquad (2\text{-}17)$$

Table 2-2. Experimental Values of the Reaction Rate Constant for the Oxidation of NO.

Reaction Rate Constant	Temperature (K)											Investigators
	273	293	298	300	303	322	333	338	352	363	372	
k_5 (atm^{-2} sec^{-1})	34.75				22.95		14.86			10.16		Bodenstein
	43.24				26.19							Hasche and Patrick
	25.9		13.4					9.75				Treacy and Daniels
				21.47								Morrison, Rinker, and Corcoran
		34.8				24.1			18.2		15.0	Greig and Hall

Sources:

1. M. Bodenstein, Z. Elektrochem. 24: 183 (1918).
2. R. L. Hasche and W. A. Patrick, J. Am. Chem. Soc. 46: 1207 (1925).
3. J. C. Treacy and F. Daniels, J. Am. Chem. Soc. 77: 2033 (1955).
4. M. E. Morrison, R. C. Rinker, and W. H. Corcoran, Ind. Eng. Chem., Fundam. 5: 175 (1966).
5. J. D. Greig and P. G. Hall, Trans. Faraday Soc. 63: 655 (1967).

Table 2-3. Henry's Law Constants at 298 K.

Species	H_i ($m^3 \cdot atm\ kg \cdot mol^{-1}$)
NO	518.0[a]
NO_2	142.9[b]
N_2O_3	2.59[c]
N_2O_4	0.769[d]
HNO_2	0.0305[e]
HNO_3	8.2×10^{-13}[f]

[a]A. G. Loomis, International Critical Tables III, 255 McGraw Hill, New York (1928).

[b]Y. N. Lee and S. E. Schwartz, J. Phys. Chem. 85: 840 (1981).

[c]C. E. Corriveau, Jr., Master's Thesis in Chemical Engineering, University of California, Berkeley (1971).

[d]H. Kramers, M. P. P. Blind, and E. Snoeck, Chem. Eng. Sci. 14: 115 (1961).

[e]E. Abel and E. Neusser, Monatsh. Chem. 54: 855 (1929).

[f]P. J. Hoftyzer and F. J. G. Kwanten, Processes for Air Pollution Control, 2nd ed., Chemical Rubber Co., Cleveland (1972).

$$N_2O_{4(g)} \rightleftharpoons N_2O_{4(l)} \qquad (2\text{-}18)$$

$$HNO_{2(g)} \rightleftharpoons HNO_{2(l)} \qquad (2\text{-}19)$$

$$HNO_{3(g)} \rightleftharpoons HNO_{3(l)} \qquad (2\text{-}20)$$

This work uses the more recent value for the NO_2 Henry's Law constant (Lee and Schwartz, 1981).

Liquid phase reactions. The important mechanisms in the liquid phase are expressed by these three reactions:

$$2NO_2 + H_2O \xrightarrow{k_6} HNO_3 + HNO_2 \qquad (2\text{-}21)$$

$$N_2O_4 + H_2O \xrightarrow{k_7} HNO_3 + HNO_2 \qquad (2\text{-}22)$$

$$N_2O_3 + H_2O \xrightarrow{k_8} 2HNO_2 \qquad (2\text{-}23)$$

The reaction of NO_2 and H_2O is slow enough to be considered a bulk phase reaction (Andrews and Hanson, 1961). It is much slower than the hydrolysis of N_2O_4 and N_2O_3, which take place in the liquid film.

Many investigators have confirmed that the rate controlling step for NO_2 absorption is the absorption and fast hydrolysis of N_2O_4. The absorption rate in the

liquid film as defined by the film theory (Danckwerts, 1970) is then,

$$R^*_{NO_2} = 2 \left(\frac{\sqrt{Dk_7}}{H}\right)_{N_2O_4} P^*_{N_2O_4} \qquad (2\text{-}24)$$

Values for the group of constants $\left(\frac{\sqrt{Dk_7}}{H}\right)_{N_2O_4}$ are given in Table 2-4. The following correlation represents the data of Hoftyzer and Kwanten (1972) for the temperature range of 276-348 K:

$$\log \left(\frac{\sqrt{Dk_7}}{H}\right)_{N_2O_4} = {}^{-}0.52 - \left(\frac{760.}{T(K)}\right) \qquad (2\text{-}25)$$

In this work, values of $\left(\frac{\sqrt{Dk_7}}{H}\right)_{N_2O_4}$ were interpolated from the work of Kramers et al. (1961), probably the best values available in the literature (Kameoka and Pigford, 1976).

The hydrolysis of N_2O_3 was studied by Corriveau (1971). A value of $1.59*10^{-3}$ kgmol/m^2·atm·s was obtained for $\left(\frac{\sqrt{Dk_8}}{H}\right)_{N_2O_3}$; k_8 and $H_{N_2O_3}$ were found to be $1.2*10$ s^{-1} and 0.39 kgmol/m^3 - atm respectively.

Table 2-4. Values of Terms in Equation (2-24) at the Various Temperatures Used in Studying the Absorption of N_2O_4 into Water.

Term	Temperature (K) 293	298	303	308	313	Investigators
$\left(\frac{\sqrt{Dk_7}}{H}\right)_{N_2O_4}\left(\frac{kg\cdot mole}{atm\ m^2\ s}\right)$		5.8×10^{-4}			5.4×10^{-4}	Wendell and Pigford
		1.1×10^{-3}		1.1×10^{-3}		Dekker, Snoeck, and Kramers
	7.7×10^{-4}		8.9×10^{-4}			Kramers, Blind, and Snoeck
		$1.0\text{-}1.1 \times 10^{-3}$				Gerstacker
		0.903×10^{-4}				Hoftyzer and Kwanten
		5.7×10^{-4}				Corriveau
		6.85×10^{-4}				Kameoka and Pigford
$k_7(s^{-1})$		290.0			1340.0	Wendell and Pigford
		290.0				Moll
	1.0×10^3					Grätzel, Henglein, Lilie, and Beck
	250.0		330.0			Kramers, Blind, and Snoeck
$H\left(\frac{atm\ m^3}{kg\cdot mole}\right)$		1.04			2.86	Wendel and Pigford

Table 2-4 (Continued)

Term	Temperature (K) 293	298	303	308	313	Investigators
	0.72		0.81			Kramers, Blind, and Schnoeck
$D\left(\frac{m^2}{s}\right)$	1.23×10^{-9}		1.59×10^{-9}			Kramers, Blind, and Schnoeck

Sources:

1. M. M. Wendle and R. L. Pigford, AIChE J. 4: 249 (1958)

2. W. A. Dekker, E. Snoeck, and H. Kramers, Chem. Eng. Sci. 14: 115 (1961).

3. H. Kramers, M. P. P. Blind, and E. Snoeck, Chem. Eng. Sci. 14:115 (1961).

4. Gerstacker, Chem. Eng. Sci. 14: 124 (1961).

5. P. J. Hoftyzer and F. J. G. Kwanten, Processes for Air Pollution Control, 2nd ed., p. 164, Chemical Rubber Company, Cleveland (1972).

6. C. E. Corriveau, Master's Thesis in Chemical Engineering, University of California, Berkeley (1971).

7. Y. Kameoka and R. L. Pigford, Ind. Eng. Chem. Funda. 16: 163 (1977).

8. A. J. Moll, Ph.D. Dissertation, University of Washington (1966).

9. M. Grätzel, A. Henglein, A. Lilie, and G. Beck, Ber. Bunsengles. 73, 646 (1969).

Structured Packings

Structured packings are a relatively new product (Bomio, 1979) on the chemical engineering market and are beginning to compete seriously with dumped packings (randomly placed rings and saddles) in the industries' separation processes. Their gain in popularity is due mainly to their high mass-transfer efficiencies, low pressure drops, and recent price drops. The market for structured packings was formerly limited to pharmaceuticals and speciality chemicals. However, the aforementioned price drops have opened up the ethlyene/styrene separation process, vacuum petroleum processes, and fatty/rosin acids separations.

These dramatic price drops (from ~ $250/ft down to ~ $100/ft) are the result of increased competition between the packings' manufacturers. The three currently recognized major producers are Koch/Sulzer, which began in the late 1960s and later developed the Flexipac packing; Glitsch, which began in 1982 and now offers the Goodloe, Metpack, and Gempack versions; Nutter, a new company (1984) based in Tulsa, Arizona, with technology licensed from Julius Montz GmbH (West Germany).

These new structured packings provide a lower pressure drop than conventional dumped packings. This can result in tremendous energy savings and higher product yield,

depending on the thermodynamics and chemical system involved. The packings also perform well in towers which require many theoretical stages, as in difficult separation processes. This can save time and money in the area of structural and material costs.

Impressive claims are made by the manufacturers concerning the mass-transfer efficiencies of their products. Factors influencing efficiency include packing depth, liquid flow rate, and column diameter. The unique structure of the packing is the key to a well-distributed liquid flow rate throughout the column, helping to eliminate dry spots which frequently occur with dumped packings. This is particularly true as liquid rate is lowered or as tower size is increased.

The manufacturers of dumped packing materials counter that their products are still the preferred choice in high pressure applications, such as ethylene service. They also maintain that dumped packings will continue to dominate the market in the forseeable future.

In choosing a packing material, it is apparent that the engineer should base his final decision on liquid loading and pressure drop pertinent to his chemical system. The general view of the industry, however, is that the structured packings will continue to carve out a larger share of the market as they become more familiar.

The column packing used in these experiments is the Koch/Sulzer Type BX packing. This packing is available in 0.15-m high sections and is constructed from a mixed fabric woven from polypropylene and acrylonitrile. This material has very good chemical stability.

Listed below are the important characteristics of the Type BX plastic packing:

1. Low pressure drop
2. Low liquid loading capability
3. High flexibility of gas loading
4. Good self-wetting properties
5. Good chemical resistance

The geometric structure of the plastic packing is the basis for the first four properties. The regularly structured cylindrical packing elements form crossing, including flow passages which are rotated by 90° to each other. This results in a good self-wetting flow pattern which in turn allows the liquid loading to be lowered. Low liquid rates reduce energy costs associated with pumping and processing the liquid.

Low pressure drop results from the fact that the gas is not required to contribute turbulence to the liquid phase. Since the gas energy requirements are lower, the pressure drop is lowered and the flexibility of the gas loading is increased. The packings chemical resistance is comparable to 100% polypropylene.

The Koch/Sulzer plastic packing is well suited for absorption processes in water, acid, or basic solutions. Such applications might be the absorption of ammonia, hydrogen chloride, sulphur dioxide, or, as in these experiments, nitrogen oxides. This packing is also useful for absorbing water-soluble solvents such as acetone, acrylonitrile, methyl alcohol, ethyl alcohol, dimethylformamide, and formaldehyde. Considering structured packings obvious advantages over dumped packings, it seems inevitable that they will be applied to many other processes in the future.

Recent Literature Concerning Low Concentration NO_2 Absorption

This section of the literature review will focus on the results of previous investigations where the absorption of low gaseous NO_2 concentrations were studied. Studying their conclusions should be a prerequisite to analyzing the experimental data of this work. It will also be important in the model development of Chapter III.

Andrews and Hanson (1961) studied NO_2 absorption using a recirculating liquid phase and a single-sieve-tray column. The temperature was maintained at 298 K and the partial pressure of NO_2^* was varied up to 0.01 atm. They concluded that at high gaseous concentrations (NO_2 > 5.0×10^{-4} kgmol/m^3), the absorption/hydrolysis of N_2O_4

is the predominant mechanism. At NO_2^* concentrations below 0.5×10^{-4} kgmol/m^3, the predominant mechanism depended on the NO/NO_2 ratio in the gas phase. When the NO/NO_2 ratio is less than 0.5 (which applies to this work), the predominant mechanism was the absorption of NO_2. At intermediate concentrations a combination of mechanisms controlled the absorption rate.

Lee and Schwartz (1981) studied the absorption of NO_2^* into water at low partial pressures. Their gas-liquid reactor consisted of a cylindrical vessel with a fritted disk as the bottom surface, through which the gas was introduced as very small bubbles. The NO_2^* concentration was varied from 8.0×10^{-4} to 1.0×10^{-7} atm. They concluded that NO_2 absorption became an important transport mechanism at the lower NO_2^* concentrations. Values for the NO_2 Henry's law constant and the second-order rate constant for NO_2 hydrolysis were determined to be 7×10^{-3} kgmol/m^3-atm and 1×10^8 m^3/kgmol-sec, respectively, at 295 K.

Koniyama and Inoue (1981) studied the absorption of NO_2 and $NO\text{-}NO_2$ mixtures into weak alkaline solutions. Their gas-liquid contactors were a bubbling absorber and a flat surface absorber. Liquid-phase mass transfer coefficients were determined by the absorption of CO_2. The NO_2 concentrations varied from 10 to 5000 ppm. They

found that the NO_2 absorption rate dependency was second order with respect to NO_2 above around 800 ppm. As NO_2 concentrations were lowered, the rate dependency changed to 3/2 order and eventually to first order. They concluded that the absorption of NO_2 became significant relative to the hydrolysis of N_2O_4 at the lower concentrations.

Literature Summary

The important species in the absorption of nitrogen oxides are NO, NO_2, N_2O_3, N_2O_4, HNO_2, HNO_3, and H_2O. Reactions (2-1), (2-2), (2-3), and (2-5) describe the gas-phase reactions.

$$2NO_2 \overset{K_1}{\rightleftharpoons} N_2O_4 \qquad (2\text{-}1)$$

$$NO + NO_2 \overset{K_2}{\rightleftharpoons} N_2O_3 \qquad (2\text{-}2)$$

$$NO + NO_2 + H_2O \overset{K_3}{\rightleftharpoons} 2HNO_2 \qquad (2\text{-}3)$$

$$2NO + O_2 \overset{k_5}{\longrightarrow} 2NO_2 \qquad (2\text{-}5)$$

The solubilities of the various species in water range from very soluble to very insoluble. In order of increasing solubility, these species are listed as NO,

NO_2, N_2O_3, N_2O_4, HNO_2, and HNO_3. The importance of these solubilities is overshadowed by the fast hydrolysis of N_2O_4 and N_2O_3.

Reactons (2-21) through (2-23) occur in the liquid phase. The hydrolysis of N_2O_4 and N_2O_3 are fast reactions that occur in the liquid film. The hydrolysis of NO_2 is much slower and is considered a bulk phase reaction.

$$2NO_2 + H_2O \xrightarrow{k_6} HNO_3 + HNO_2 \qquad (2\text{-}21)$$

$$N_2O_4 + H_2O \xrightarrow{k_7} HNO_3 + HNO_2 \qquad (2\text{-}22)$$

$$N_2O_3 + H_2O \xrightarrow{k_8} 2HNO_2 \qquad (2\text{-}23)$$

Application of the theory of absorption with chemical reaction (Danckwerts, 1970) was of tremendous help to the study of NO_x absorption.

The Koch/Sulzer Type BX packing is suited well for aqueous absorption processes. The low pressure drop, low liquid loading capability, and good chemical resistance of the packing should work well with the NO_x system. The packing's ability to remove gaseous nitrogen oxides should be important information for future NO_x absorption studies.

The nature of NO_x absorption is not completely understood, especially at the lower concentrations where air pollution studies are involved. Literature values for the NO_2 Henry's law constant are not consistent and the degree of importance of the mechanisms involved are not clearly defined. In light of the current literature however, it is becoming more apparent that the absorption of the NO_2 specie should be treated as an important mechanism at low NO_2 concentrations.

CHAPTER 3

MODEL DEVELOPMENT

Two absorption models are proposed in this work in an effort to describe the experimental data. Owing to the complex reactions involved a simple approach was initially taken in the model development. The first model considered the absorption/fast hydrolysis of the derivation being shown in Appendix D:

$$(Y^{*}_{NO_2,OUT})^{-1} - (Y^{*}_{NO_2,IN})^{-1} = \frac{2\left(\frac{\sqrt{Dk_7}}{H}\right) P_T K_1 a_i Z}{G'} \quad (3\text{-}1)$$

A brief explanation of why this model was not used is in order. During the analysis of the data interfacial areas for each individual run were calculated from Equation (3-1). It was found that the interfacial area appeared to be a function of the NO_2 concentration in the gas phase. Since the interfacial area should be primarily a function of liquid rate and packing properties only, it appeared that another mechanism was present. Consequently, this model was rejected.

The second and more effective model proposes the absorption/hydrolysis of N_2O_4 along with the physical absorption of the NO_2 specie. The assumptions of this second model are:

1. Only liquid phase resistance is present.
2. The column operates in the plug flow regime with respect to gas and liquid flow.
3. Decomposition of aqueous HNO_2 is negligible.
4. Gases behave ideally.
5. No oxidation of gaseous NO.
6. Partial pressure of NO_2 is approximately equal to the partial pressure of NO_2^*.

The modeling begins with a basic flux equation,

$$-G'(dY_{NO_2}^*) = N_{NO_2}^* a_i dz \tag{3-2}$$

The flux of NO_2^* is then defined as,

$$N_{NO_2}^* = 2\left(\frac{\sqrt{Dk_7}}{H}\right)_{N_2O_4} P_{N_2O_4} + \left(\frac{k_L}{H_{NO_2}}\right) P_{NO_2} \tag{3-3}$$

Also, the equilibrium relationship between NO_2 and N_2O_4 is,

$$P_{N_2O_4} = K_1 (P_{NO_2})^2 \tag{3-4}$$

with the equilibrium constant K_1 being a function of temperature only. Combining Equations (3-2), (3-3), and (3-4) and assuming that $P_{NO_2} = Y_{NO_2}^* \times P_T$ gives,

$$-G'(dY_{NO_2}^*) = \left[2\left(\frac{\sqrt{Dk_7}}{H}\right)_{N_2O_4} K_1 (Y_{NO_2}^* P_T)^2 + \left(\frac{k_L}{H_{NO_2}}\right) Y_{NO_2}^* P_T \right] a_i dz \qquad (3\text{-}5)$$

After dividing by G', the following definitions are made and substituted into Equation (3-5). The result is Equation (3-8):

$$A = \left(\frac{k_L P_T}{G' H_{NO_2}}\right) \qquad (3\text{-}6)$$

$$B = 2\left(\frac{\sqrt{Dk_7}}{H}\right)_{N_2O_4} K_1 \left(\frac{P_T^2}{G'}\right) \qquad (3\text{-}7)$$

$$-d(Y_{NO_2}^*) = \left[BY_{NO_2}^{*2} + AY_{NO_2}^* \right] a_i dz \qquad (3\text{-}8)$$

This equation can be separated and integrated to give the model's working equation,

$$-\int_{Y_{IN}}^{Y_{OUT}} \frac{dY_{NO_2}^*}{(BY_{NO_2}^* + A) Y_{NO_2}^*} = a_i \int_0^Z dz \qquad (3\text{-}9)$$

$$\frac{1}{A} \ln \frac{A + BY}{Y} \Bigg|_{Y_{IN}}^{Y_{OUT}} = a_i Z \qquad (3\text{-}10)$$

$$\frac{1}{A}\left[\ln\frac{A + BY_{OUT}}{Y_{OUT}} - \ln\frac{A + BY_{IN}}{Y_{IN}}\right] = a_i Z \qquad (3\text{-}11)$$

Resubstituting for the defined variables A and B and rearranging to solve for a_i gives the final form of the model equation,

$$a_i = \left(\frac{H_{NO_2} G'}{k_L P_T Z}\right)\left[\ln\frac{\left(\frac{k_L P_T}{G' H_{NO_2}}\right) + 2\left(\frac{\sqrt{Dk_7}}{H}\right)_{N_2O_4} K_1\left(\frac{P_T^2}{G'}\right) Y^*_{NO_2,OUT}}{Y^*_{NO_2,OUT}} - \ln\frac{\left(\frac{k_L P_T}{G' H_{NO_2}}\right) + 2\left(\frac{\sqrt{Dk_7}}{H}\right)_{N_2O_4} K_1\left(\frac{P_T^2}{G'}\right) Y^*_{NO_2,IN}}{Y^*_{NO_2,IN}}\right] \qquad (3\text{-}12)$$

Values for all the variables in this equation can be found either in the literature or from experimental data, except k_L and a_i. k_L and a_i will be determined by data analysis.

CHAPTER 4

EXPERIMENTAL APPARATUS AND PROCEDURE

The flowsheet of the experimental equipment is shown in Figure 4-1. The NO_x scrubber is a packed column using Koch/Sulzer (Type BX) packing. The column is constructed of 0.1016 m-ID Pyrex glass pipe. The packing elements are 0.15 m long and are packed to a height of 0.80 m. Flanges and piping are of stainless steel.

Process air and water supply systems are available. The liquid rate is metered by a Fisher-Porter (Model 10 A 1755) rotameter. The gas phase equipment includes a Brooks (IC 03835) air-rotameter, a Whitey (SS-22RS4) micrometering valve, a Beckman NO_x/NO gas analyzer (Model 951), a calibration gas supply system, and an exhaust gas system. The main gas and liquid flow lines are made of 0.0254 m-OD and 0.0127 m-OD stainless steel piping, respectively. Gas sample lines are 0.0064 m-OD stainless steel tubing.

The Beckman chemiluminescent gas analyzer is specific for NO and NO_x (NO_2^* + NO) measurements. It requires one hour to warm up before operating. It is calibrated using process air (for zero calibration) and standard NO and NO_2^* gas tanks of known commercial purity (2200 ppm and 2140 ppm, respectively) before each series of runs. After

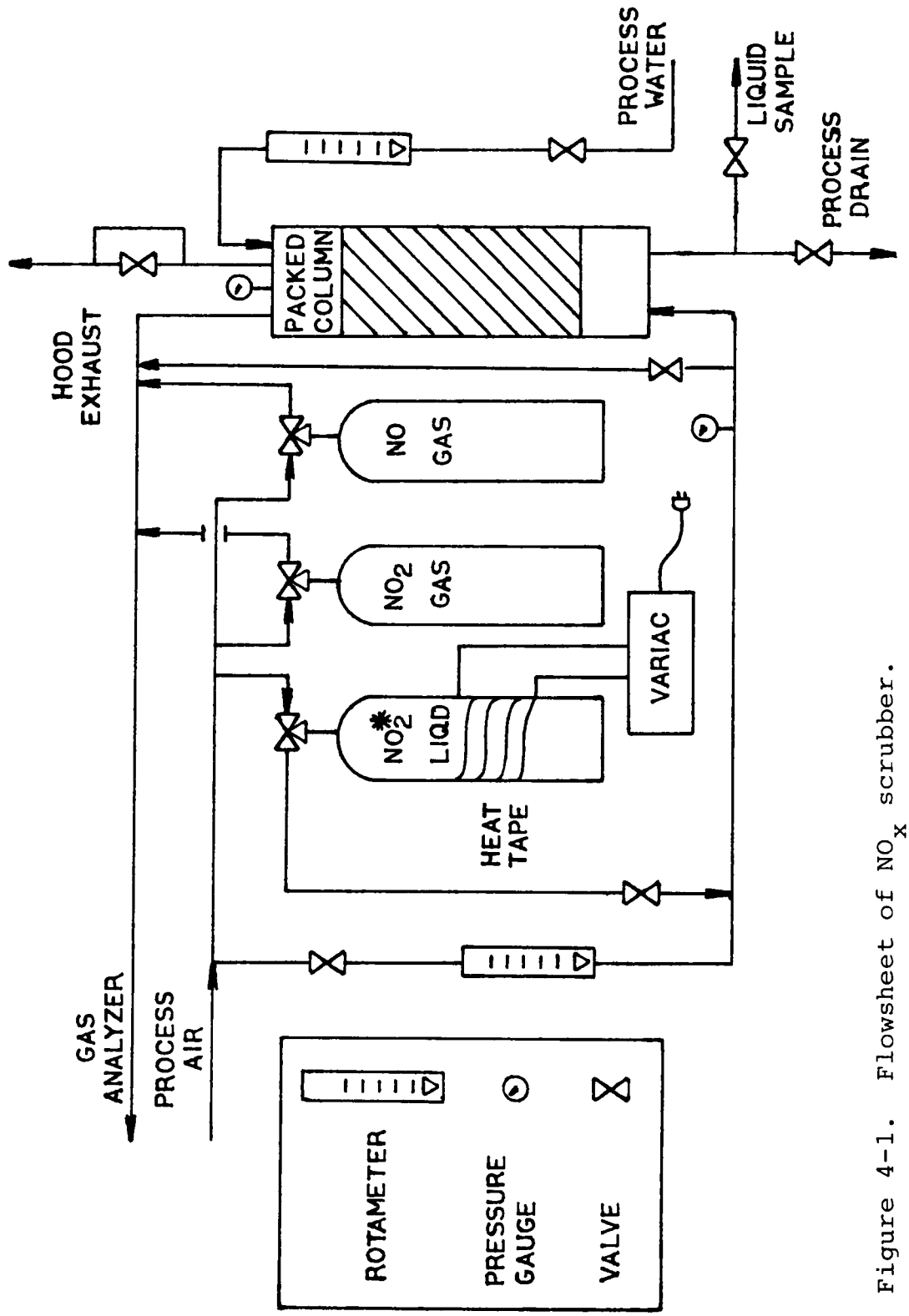

Figure 4-1. Flowsheet of NO_x scrubber.

initial calibration, future calibrations are quickly made as little adjustment is needed. Normal operation of the system begins with adjusting the water and air to the desired flow rates using the rotameters. The liquid rotameter allows a maximum flow of 4.2 LPM. The air rotameter allows a maximum flow of 380.0 LPM, although the available process air is limited to approximately 240.0 LPM. Gaseous NO_2^* ($NO_2 + 2N_2O_4$) is supplied to the system by vaporizing the liquid NO_2^* tank with heating tape. The amount of heat required for vaporization is estimated and then regulated with a variac. The gaseous NO_2^* is metered by a three-way pressure regulator and a Whitey micrometering valve. Control is such that the entire gas analyzer range (0 to 10000 ppm) can be covered.

After the inlet NO_x concentration is set, the outlet NO_x concentration is monitored to determine steady state. When the gas and liquid flow rates and the inlet and outlet NO_x concentrations show no change over a period of time, the system is said to be at steady state. The response of the system is such that steady state appears to be reached after only a few minutes, however, 15-20 minutes are allowed for each run to insure stability.

At steady state, the inlet and outlet NO and NO_x concentrations (ppm) are recorded. Liquid and gas flow rates are recorded and inlet and outlet water samples

are taken. In all runs the outlet fluid concentrations are recorded before the inlet fluid measurements are made. This is done to avoid upsetting the stability and performance of the NO_x scrubber. After these measurements are recorded, system variables are reset for the next run.

The column temperature is estimated by measuring the outlet water temperature with a thermometer. The column usually operates at 295.0 to 295.5 K, although some runs were made at 298.0 K. Total column pressure is estimated to be 1 atm since pressure gauges on the inlet and outlet flow lines register zero pressure and the system is open to the atmosphere. The inlet and outlet partial pressures of NO_2, N_2O_4, and NO_2^* are calculated from the gas analyzer readings.

The hydrogen ion concentration (H^+) in the water samples is measured using a Leeds & Northrup pH meter (CAT. 7401). The pH meter is calibrated in the acid region using standard buffer solutions of known concentration (pH=7.4, 5.0, 4.0, 3.0). The nitric and nitrous acid concentrations are calculated from the amount of NO_2^* removed from the gas and are compared to the water sample measurements.

The liquid waste stream is discharged directly to a process drain. Liquid rates above 3.0 LPM cannot

be handled by the drain because of flooding. The exhaust gas stream is routed to a hood exhaust. The entire system, including gas analyzer, operates in a fume hood for safety.

CHAPTER 5

EXPERIMENTAL RESULTS AND ANALYSIS

Presentation of Experimental Data

The steady state operating conditions of the experimental runs are presented in Table 5-1. This data includes run number, temperature (K), liquid and gas flow rates (LPM), and the inlet and outlet partial pressures (atm) of NO, NO_2, N_2O_4, NO_2^*, and NO_x. Their relationship to one another has been defined as,

$$P_{NO_2^*} = P_{NO_2} + 2P_{N_2O_4} \tag{2-6}$$

$$P_{NO_x} = P_{NO_2^*} + P_{NO} \tag{2-7}$$

A sample calculation of the partial pressure for each specie from the experimental readings is in the Appendix. The conversion of NO_2^* will be defined as,

$$X_{NO_2^*} = \frac{P_{NO_2^*,IN} - P_{NO_2^*,OUT}}{P_{NO_2^*,IN}} \tag{5-1}$$

Table 5-2 presents the conversion of NO_2^* and the interfacial area for each run. These interfacial areas were calculated from the model expressed in Equation (3-12),

Table 5-1. Steady State Operating Conditions.

Run	Temp. (K)	Gas Rate (LPM)	Liquid Rate (LPM)	Inlet Partial Pressures x 10^6 (atm)					Outlet Partial Pressures x 10^6 (atm)				
				NO	NO_2	N_2O_4	NO_2^*	NO_x	NO	NO_2	N_2O_4	NO_2^*	NO_x
1	295.0	232.2	1.3	5	145	0.1727	145	150	5	125	0.1284	125	130
2	295.0	232.2	2.12	5	140	0.161	140	145	5	120	0.1183	120	125
3	295.0	232.2	3.0	10	135	0.151	135	145	7	118	0.1144	118	125
4	295.0	232.2	1.3	55	462	1.753	465	520	50	353	1.024	355	405
5	295.0	232.2	2.12	65	462	1.753	465	530	53	360	1.065	362	415
6	295.0	232.2	3.0	65	471	1.822	475	540	55	368	1.113	370	425
7	295.0	232.2	1.3	140	873	6.26	885	1025	115	575	2.716	580	695
8	295.0	232.2	2.12	145	882	6.39	895	1040	110	589	2.85	595	705
9	295.0	232.2	3.0	155	907	6.76	920	1075	120	589	2.85	595	715
10	295.5	151.0	1.3	0	130	0.1335	130	130	0	110	0.0956	110	110
11	295.5	151.0	1.3	0	127	0.1274	127	127	0	105	0.0871	105	105
12	295.5	151.0	1.3	0	115	0.1044	115	115	0	97	0.0743	97	97
13	295.5	151.0	1.3	125	648	3.316	655	780	80	407	1.308	410	490
14	295.5	151.0	1.3	120	673	3.577	680	800	80	427	1.44	430	510
15	295.5	151.0	1.3	130	702	3.892	710	840	80	437	1.51	440	520
16	295.5	151.0	1.3	140	732	4.231	740	880	90	447	1.578	450	540
17	295.5	151.0	1.3	300	1298	13.3	1325	1625	210	648	3.32	655	865
18	295.5	151.0	1.3	280	1270	12.74	1295	1575	215	663	3.47	670	885
19	295.5	151.0	1.3	45	338	0.902	340	385	35	269	0.571	270	305
20	295.5	151.0	1.3	45	328	0.85	330	375	35	254	0.509	255	290
21	295.0	188.2	1.3	17	311	0.795	313	330	13	241	0.477	242	255
22	295.0	188.2	1.3	50	427	1.498	430	480	45	308	0.779	310	355
23	295.0	188.2	1.3	105	624	3.2	630	735	75	432	1.533	435	510
24	295.0	188.2	1.3	260	1240	12.63	1265	1525	225	712	4.165	720	945
25	295.0	188.2	1.3	215	1042	8.92	1060	1275	180	614	3.1	620	800

Table 5-1 (Continued)

Run	Temp. (K)	Gas Rate (LPM)	Liquid Rate (LPM)	Inlet Partial Pressures x 10^6 (atm)					Outlet Partial Pressures x 10^6 (atm)				
				NO	NO_2	N_2O_4	NO_2^*	NO_x	NO	NO_2	N_2O_4	NO_2^*	NO_x
26	295.0	188.2	1.3	200	936	7.2	950	1150	175	550	2.49	555	730
27	295.0	188.2	1.3	150	663	3.61	670	820	110	452	1.68	455	565
28	295.5	151.0	0.87	237	1228	11.9	1252	1488	212	607	2.91	613	825
29	295.5	151.0	1.71	250	1226	11.87	1250	1500	209	604	2.88	610	819
30	295.5	151.0	2.54	250	1226	11.87	1250	1500	212	620	3.04	626	838
31	295.5	151.0	0.87	363	1632	21.0	1674	2037	308	746	4.39	755	1063
32	295.5	151.0	1.71	350	1657	21.7	1700	2050	300	766	4.63	775	1075
33	295.5	151.0	2.54	375	1621	20.75	1662	2037	313	753	4.48	762	1075
34	295.5	151.0	0.87	450	1988	31.2	2050	2500	387	864	5.9	876	1263
35	295.5	151.0	1.71	465	1926	29.3	1985	2450	377	825	5.375	836	1213
36	295.5	151.0	2.54	475	1917	29.02	1975	2450	377	825	5.375	836	1213
37	298.0	77.2	0.87	263	1158	8.71	1175	1438	169	466	1.41	469	638
38	298.0	77.2	1.71	281	1212	9.54	1231	1512	169	503	1.64	506	675
39	298.0	77.2	2.54	312	1206	9.446	1225	1537	187	498	1.61	501	688
40	298.0	77.2	0.87	444	1646	17.6	1681	2125	300	559	2.03	563	863
41	298.0	77.2	1.71	431	1658	17.85	1694	2125	288	607	2.39	612	900
42	298.0	77.2	2.54	431	1538	15.36	1569	2000	300	571	2.118	575	875
43	298.0	77.2	0.87	550	1855	22.3	1900	2450	378	617	2.47	622	1000
44	298.0	77.2	1.71	575	1855	22.3	1900	2475	375	645	2.7	650	1025
45	298.0	77.2	2.54	600	2046	27.19	2100	2700	438	668	2.9	674	1112

Table 5-2. NO_2^* Conversion and Interfacial Area for Each Run.

Run	$X_{NO_2}^*$	$a(m^{-1}x10^{-2})$	Run	$X_{NO_2}^*$	$a(m^{-1}x10^{-2})$
1	0.138	6.97	26	0.416	8.31
2	0.143	7.33	27	0.321	7.24
3	0.126	6.46	28	0.51	7.91
4	0.237	7.57	29	0.512	7.97
5	0.222	6.98	30	0.499	7.6
6	0.221	6.87	31	0.549	7.29
7	0.345	8.13	32	0.544	7.07
8	0.335	7.75	33	0.542	7.13
9	0.353	8.19	34	0.573	6.77
10	0.154	5.34	35	0.579	7.11
11	0.173	6.15	36	0.577	7.09
12	0.157	5.64	37	0.601	6.54
13	0.374	7.48	38	0.589	6.07
14	0.368	7.12	39	0.591	6.13
15	0.38	7.27	40	0.665	6.46
16	0.392	7.4	41	0.639	5.8
17	0.506	7.45	42	0.634	6.02
18	0.483	6.96	43	0.637	6.08
19	0.206	5.04	44	0.658	5.74
20	0.227	5.77	45	0.679	5.78
21	0.227	7.26			
22	0.279	7.92			
23	0.31	7.18			
24	0.431	7.1			
25	0.415	7.65			

$$a_i = \left(\frac{H_{NO_2} G'}{k_L P_T Z}\right) \left[\ln \frac{\left(\frac{k_L P_T}{G' H_{NO_2}}\right) + 2\left(\frac{\sqrt{Dk_7}}{H}\right)_{N_2O_4} K_1 \left(\frac{P_T^2}{G'}\right) Y^*_{NO_2,OUT}}{Y^*_{NO_2,OUT}} - \ln \frac{\left(\frac{k_L P_T}{G' H_{NO_2}}\right) + 2\left(\frac{\sqrt{Dk_7}}{H}\right)_{N_2O_4} K_1 \left(\frac{P_T^2}{G'}\right) Y^*_{NO_2,IN}}{Y^*_{NO_2,IN}} \right] \quad (3\text{-}12)$$

Figure 5-1 through 5-3 show the conversion of NO_2^* versus liquid rate at various gas rates and inlet NO_2^* partial pressures. These figures show no effect of liquid rates on NO_2^* conversion, which suggests that the Koch/Sulzer packing maintains a constant wetted surface area over the range of liquid rates studied. This conclusion is in agreement with the manufacturers' claim of a constant wetted surface area (Bomio, 1979).

NO_2^* conversion versus gas rate is examined in Figure 5-4 through 5-7. Other variables include liquid rate and inlet NO_2^* partial pressure. These graphs show a general trend of decreasing conversion with increasing gas rate. This tends to be justifiable as increased gas flow reduces the contact time between the liquid and gas phases; this reduces the time available for absorption into the liquid phase, causing decreased NO_2^* conversion.

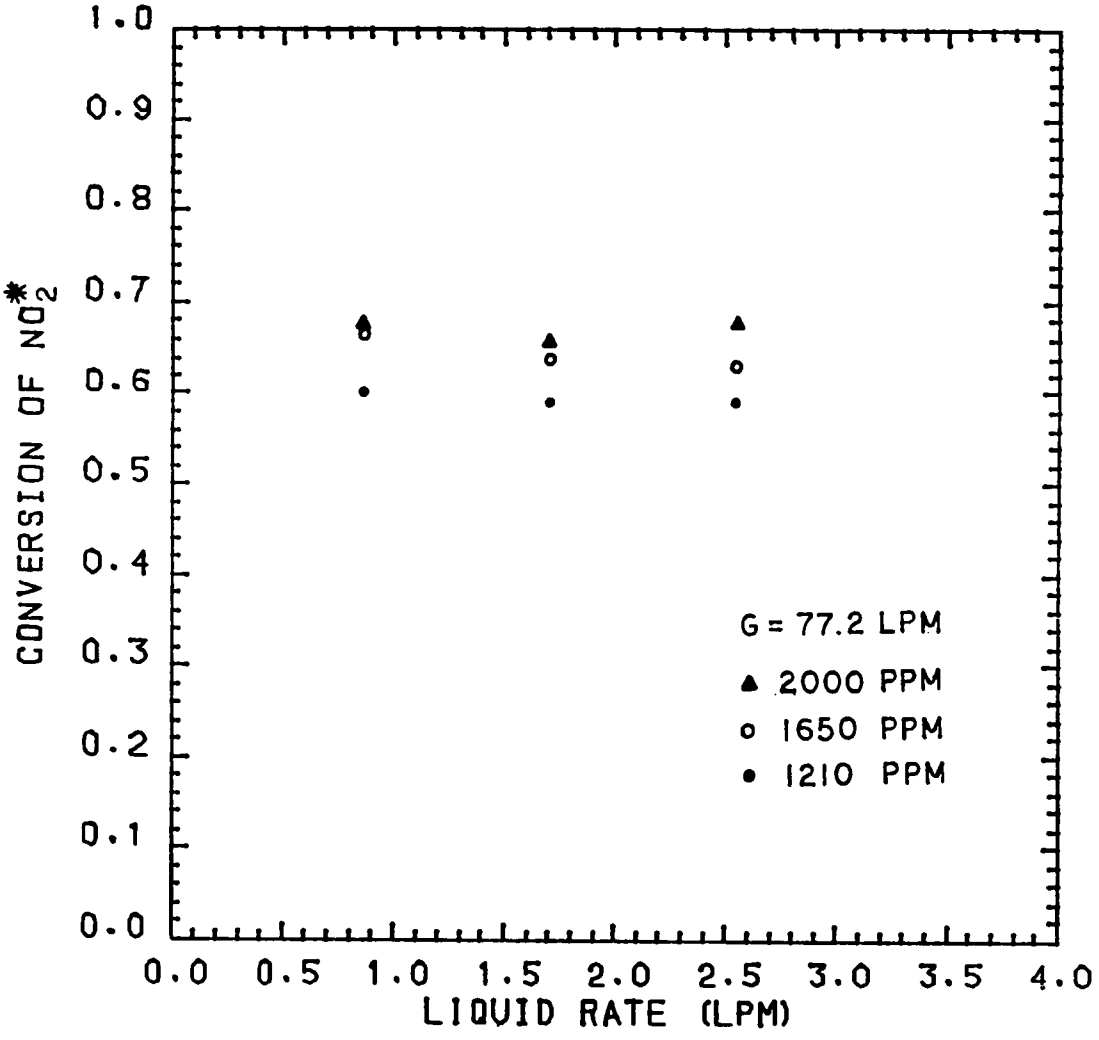

5-1. NO_2^* conversion versus liquid rate at various inlet NO_2^* concentrations--gas rate is 77.2 LPM.

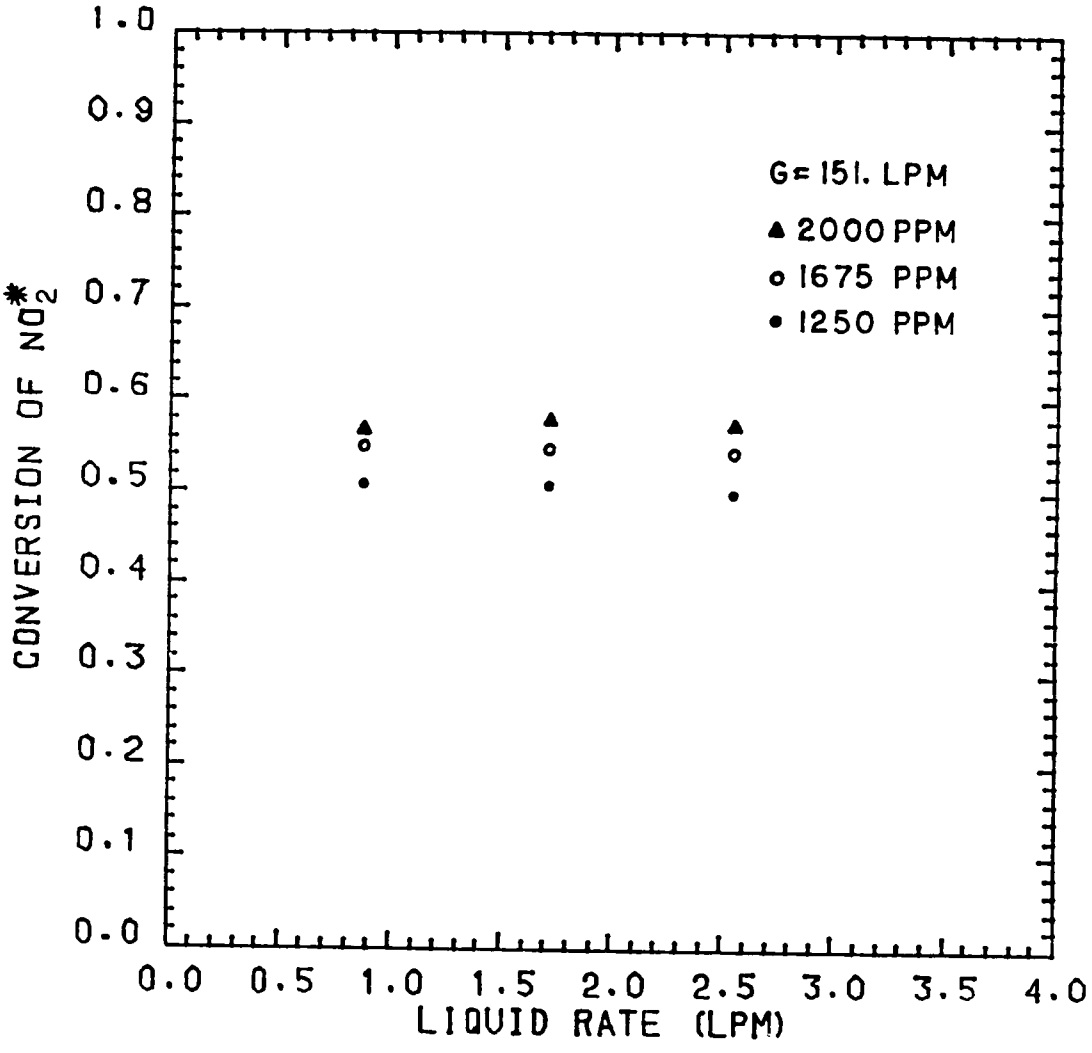

5-2. NO_2^* conversion versus liquid rate at various inlet NO_2^* concentrations--gas rate is 151.0 LPM.

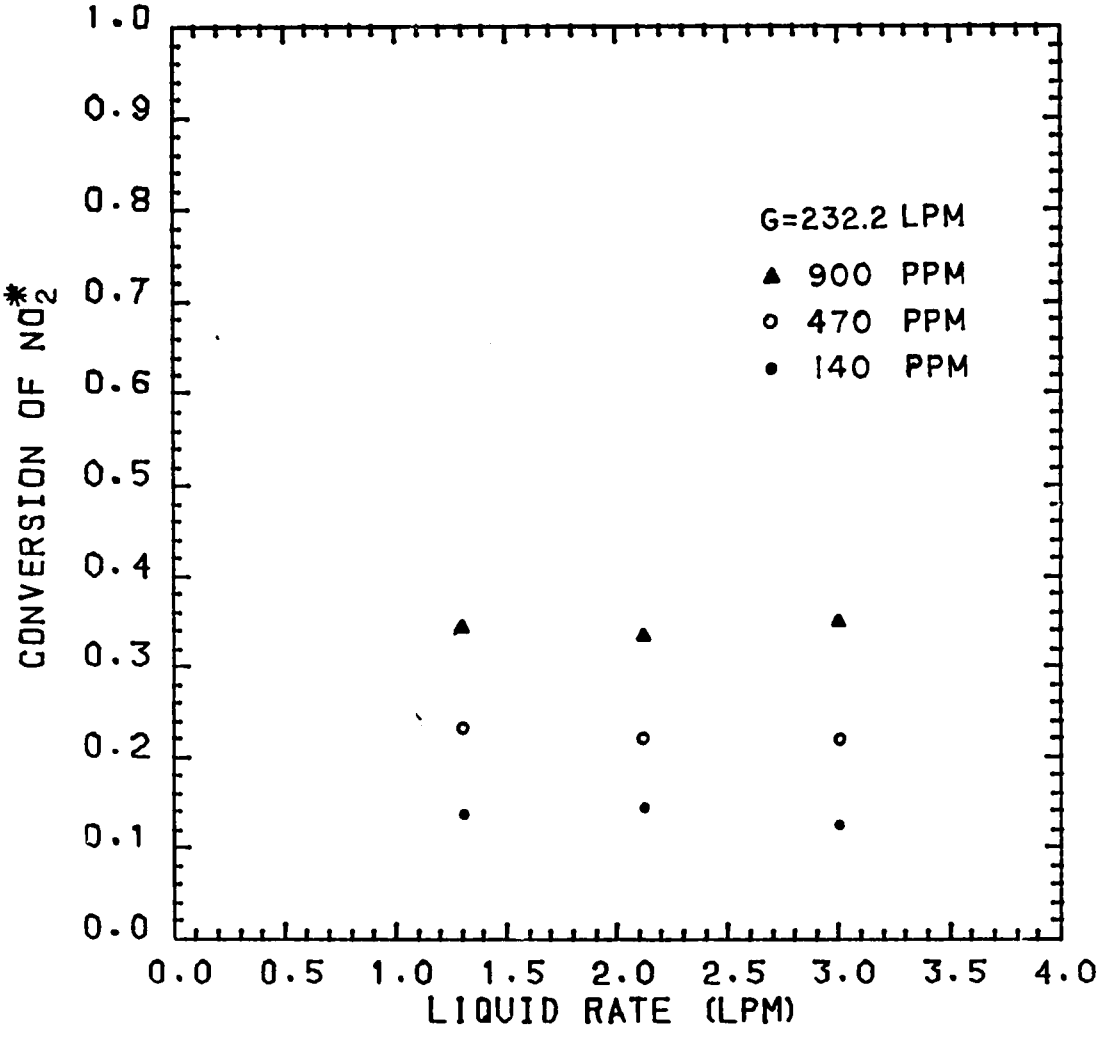

5-3. NO_2^* conversion versus liquid rate at various inlet NO_2^* concentrations--gas rate is 232.2 LPM.

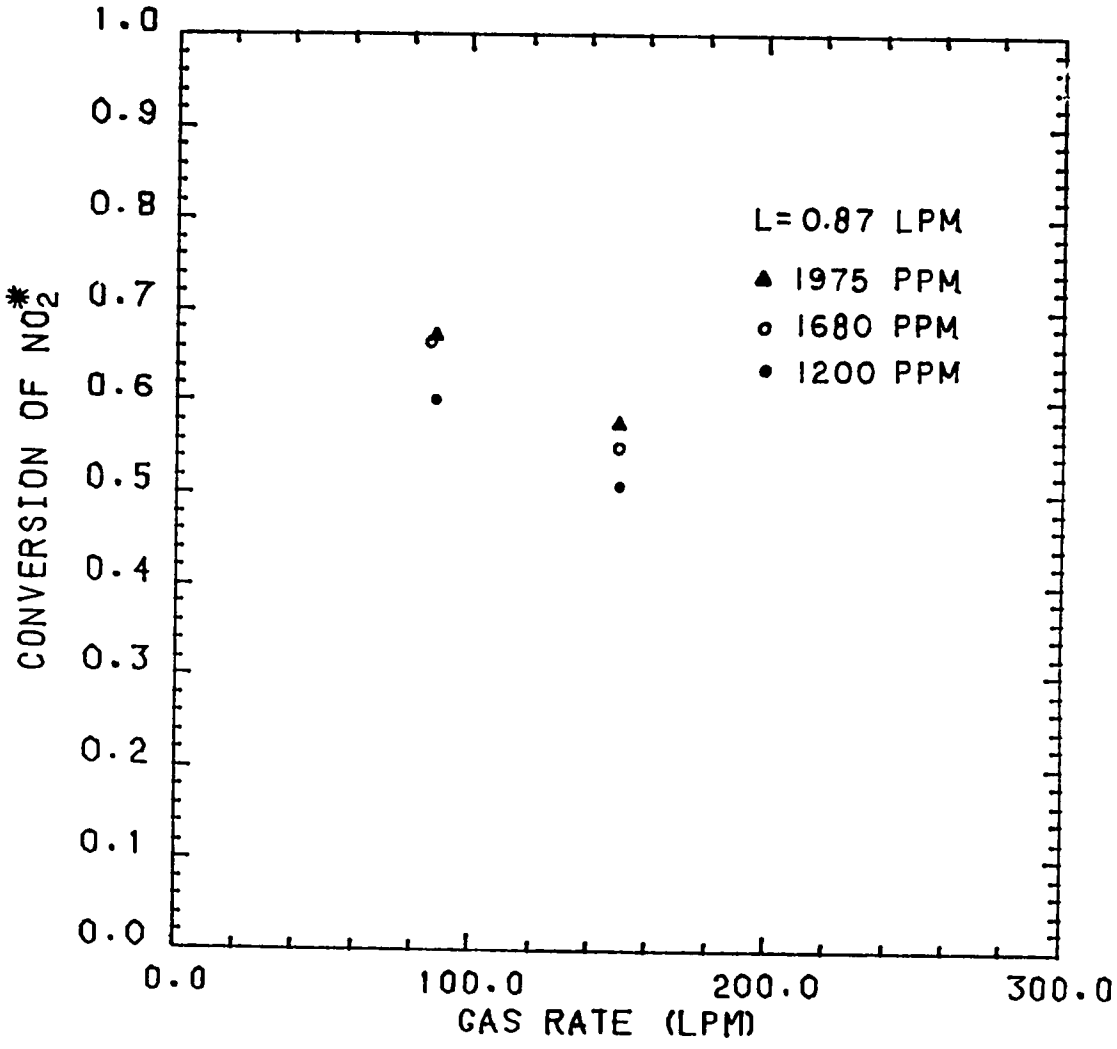

5-4. NO_2^* conversion versus gas rate at various inlet NO_2^* concentrations--liquid rate is 0.87 LPM.

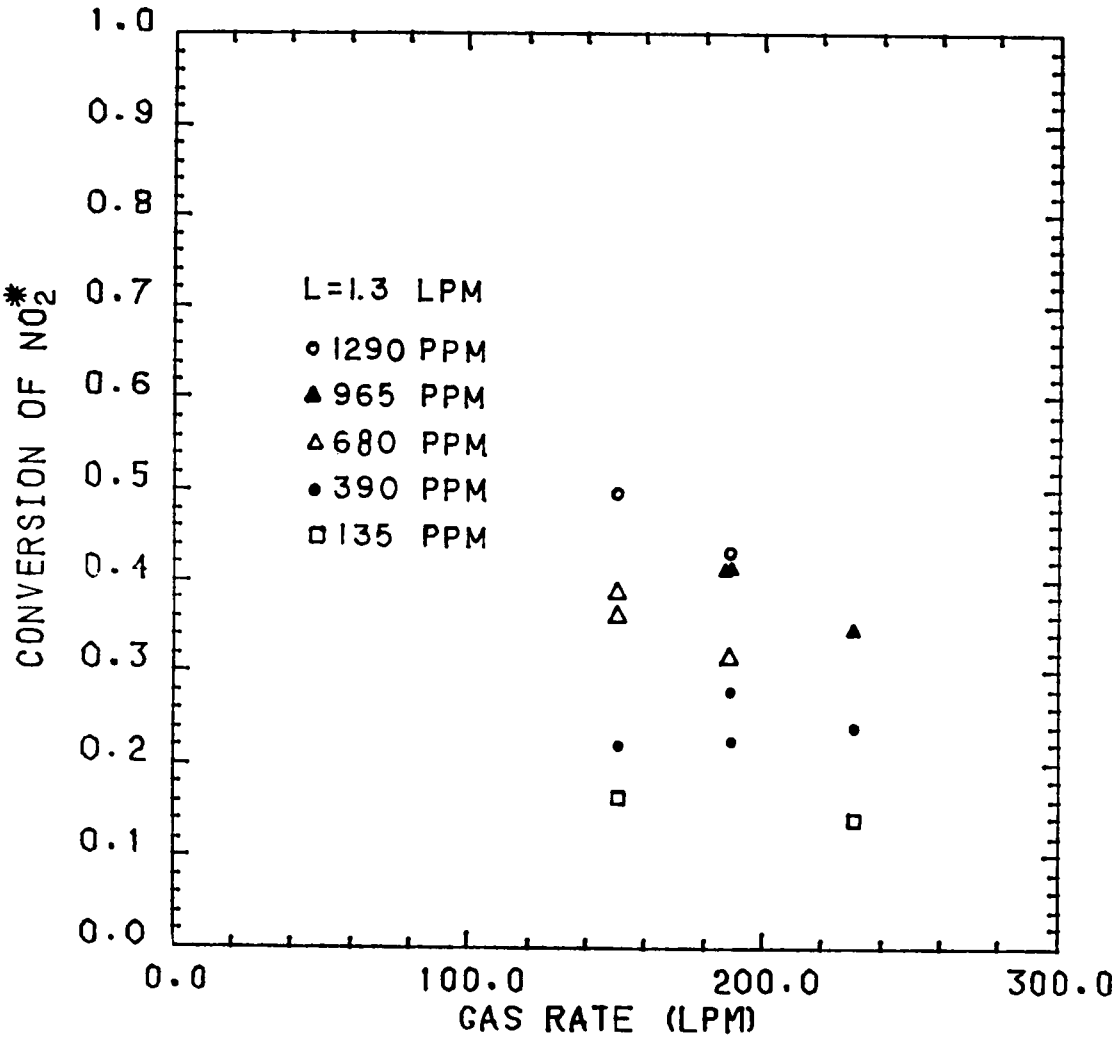

5-5. NO_2^* conversion versus gas rate at various inlet NO_2^* concentrations--liquid rate is 1.3 LPM.

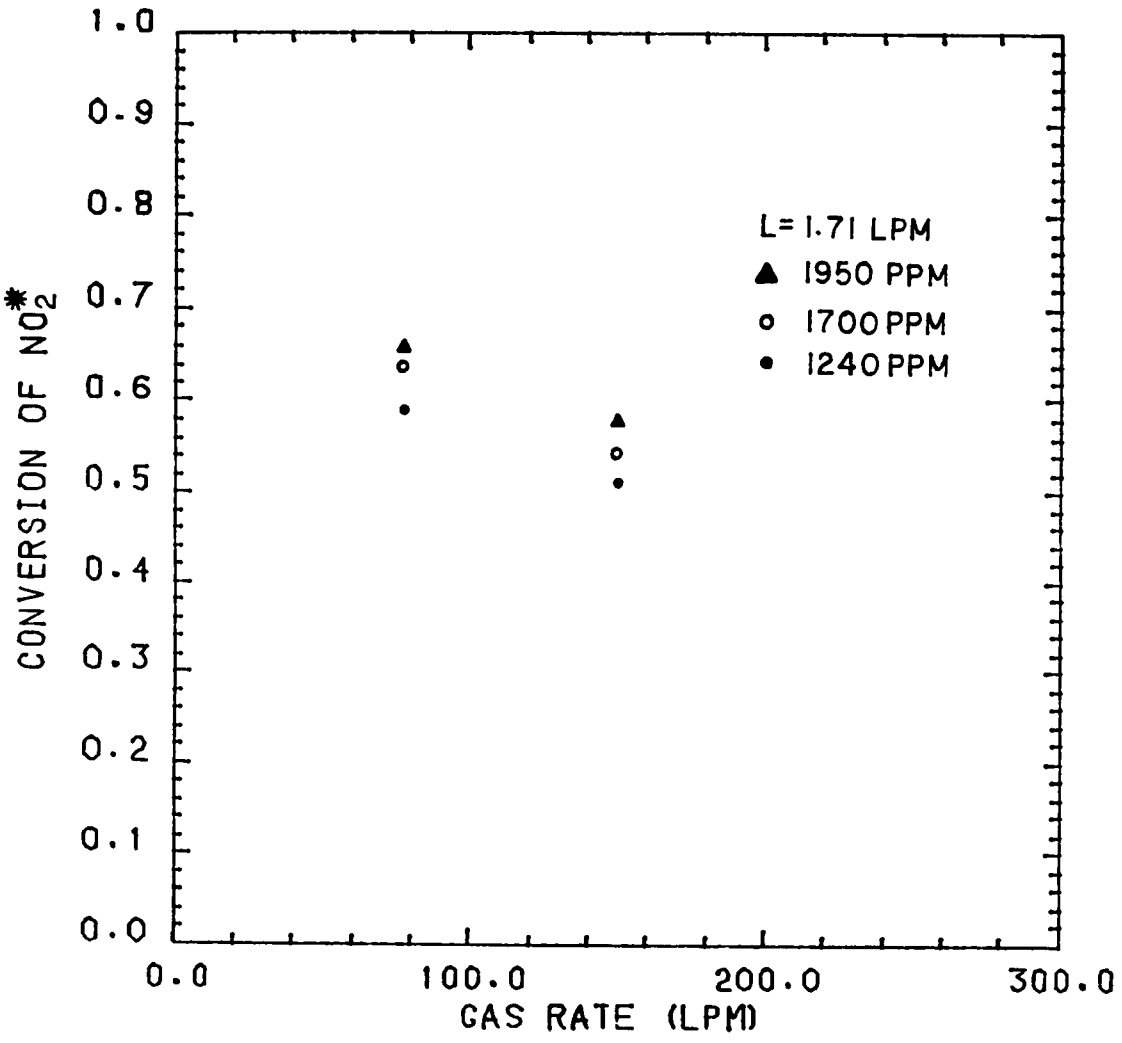

5-6. NO_2^* conversion versus gas rate at various inlet NO_2^* concentrations--liquid rate is 1.71 LPM.

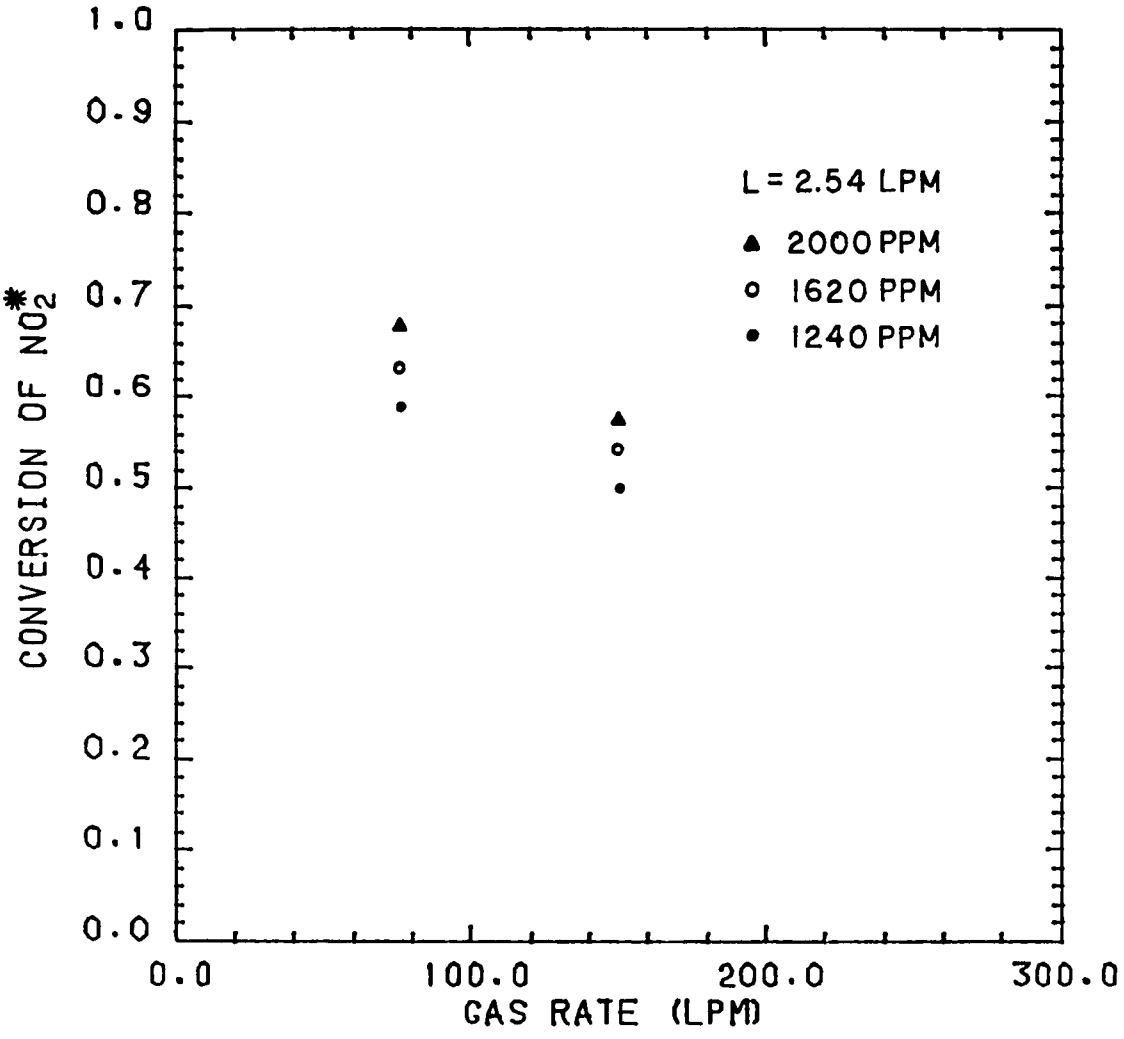

5-7. NO_2^* conversion versus gas rate at various inlet NO_2^* concentrations--liquid rate is 2.54 LPM.

Figure 5-8 shows the NO_2^* conversion versus inlet NO_2^* partial pressure. Gas rate is the only other variable shown since Figures 5-1 through 5-3 show no effect of liquid rate on NO_2^* conversion. This graph exhibits an increase in NO_2^* conversion with increasing inlet NO_2^* partial pressure. This trend is consistent with increased absorption rates at higher NO_2^* driving force partial pressures.

Analysis of Model Versus Data

The manufacturer of the packing claims that its interfacial area remains constant over a wide range of liquid rates. Utilizing this knowledge, reasonable values of k_L were chosen to generate an interfacial area for each run, from which an average interfacial area was calculated. A value of k_L which minimized the error between the average and individual interfacial areas was sought. The value of k_L was determined to be 4.982×10^{-4} m/s, giving an average interfacial area of 690. m^{-1}.

Figures 5-9 through 5-11 show the interfacial area versus liquid rate at various gas rates and inlet NO_2^* partial pressures. These graphs reveal little change in interfacial area with liquid rate at all gas rates studied, giving the same conclusion as Figures 5-1 through 5-3.

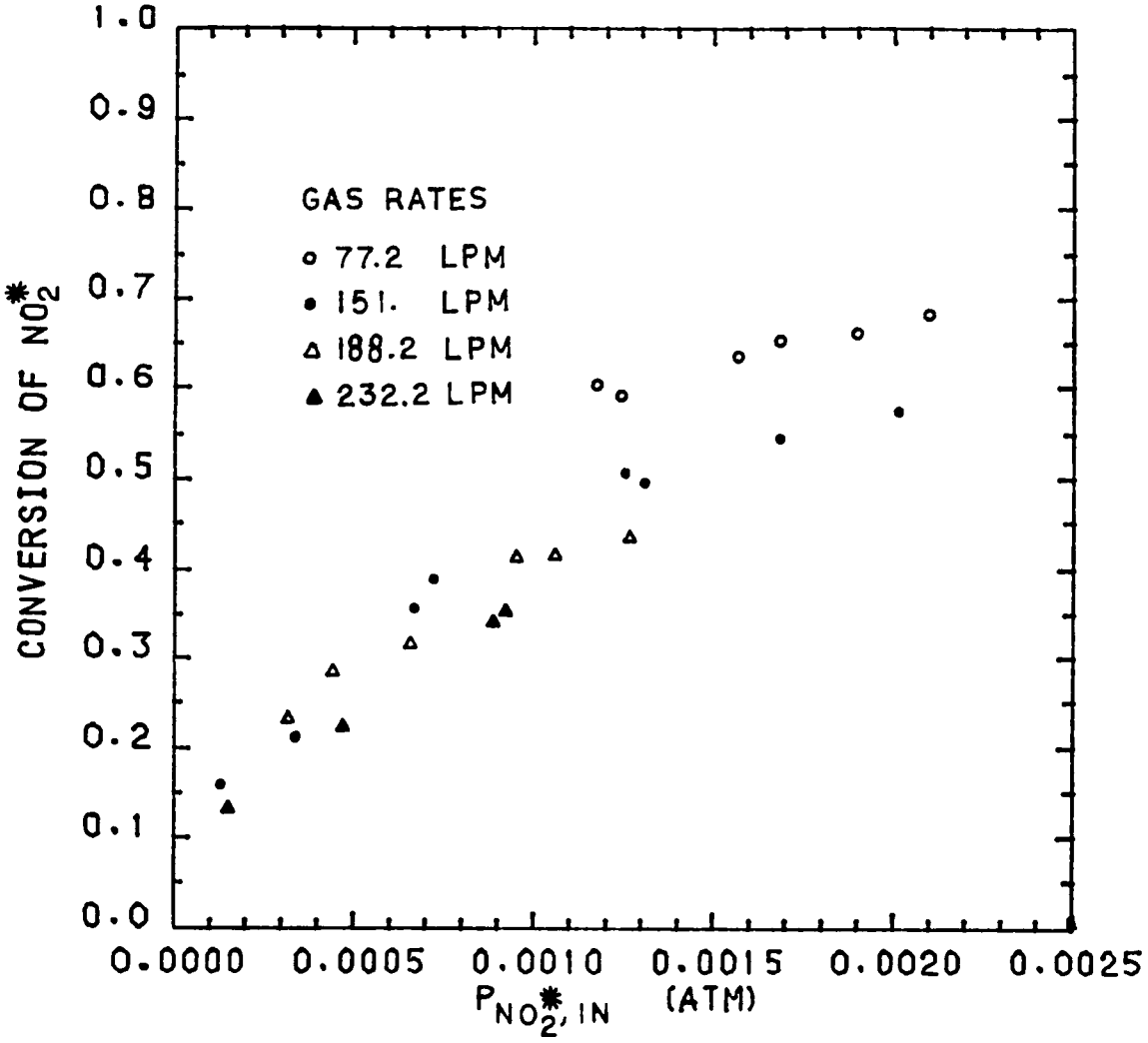

5-8. NO_2^* conversion versus inlet NO_2^* concentration at various gas rates.

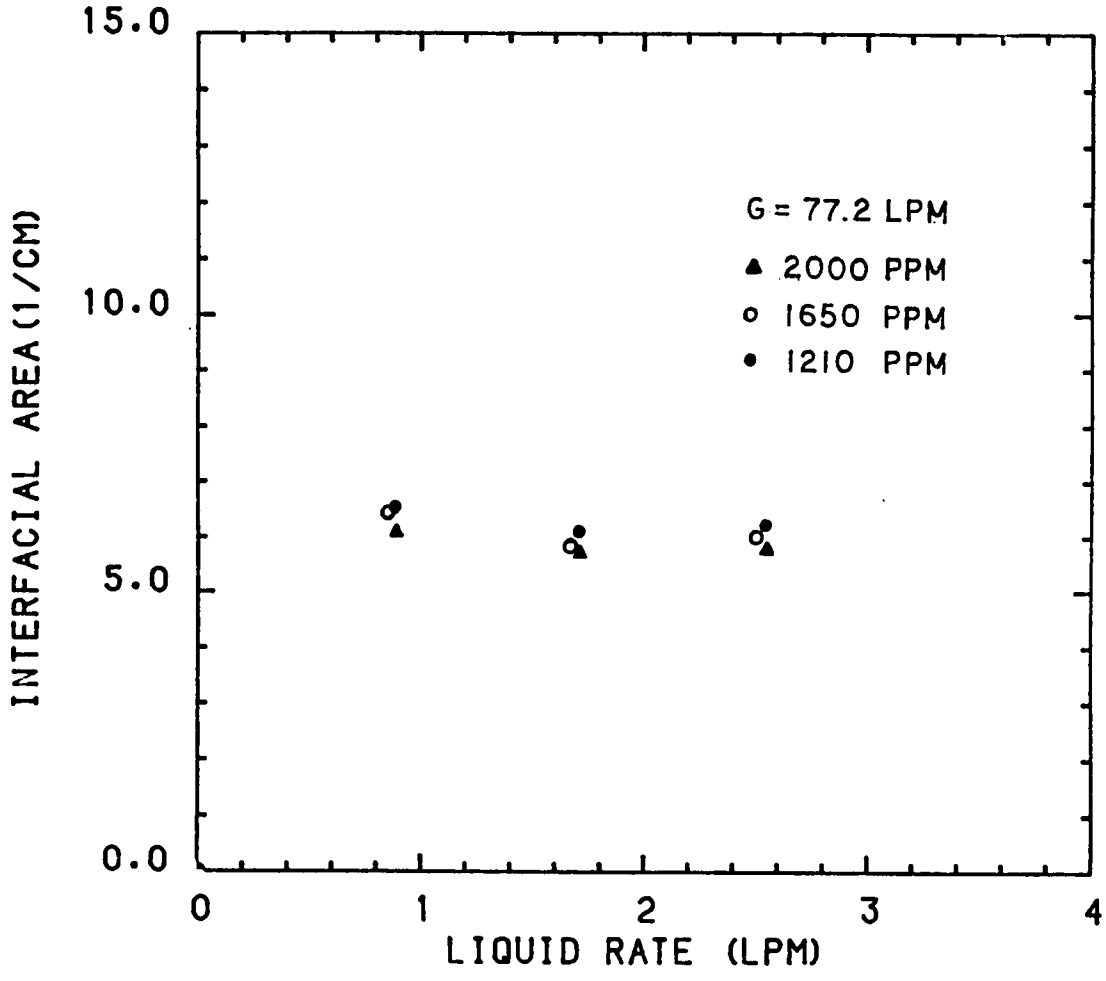

5-9. Interfacial area versus liquid rate at various inlet NO_2^* concentrations--gas rate is 77.2 LPM.

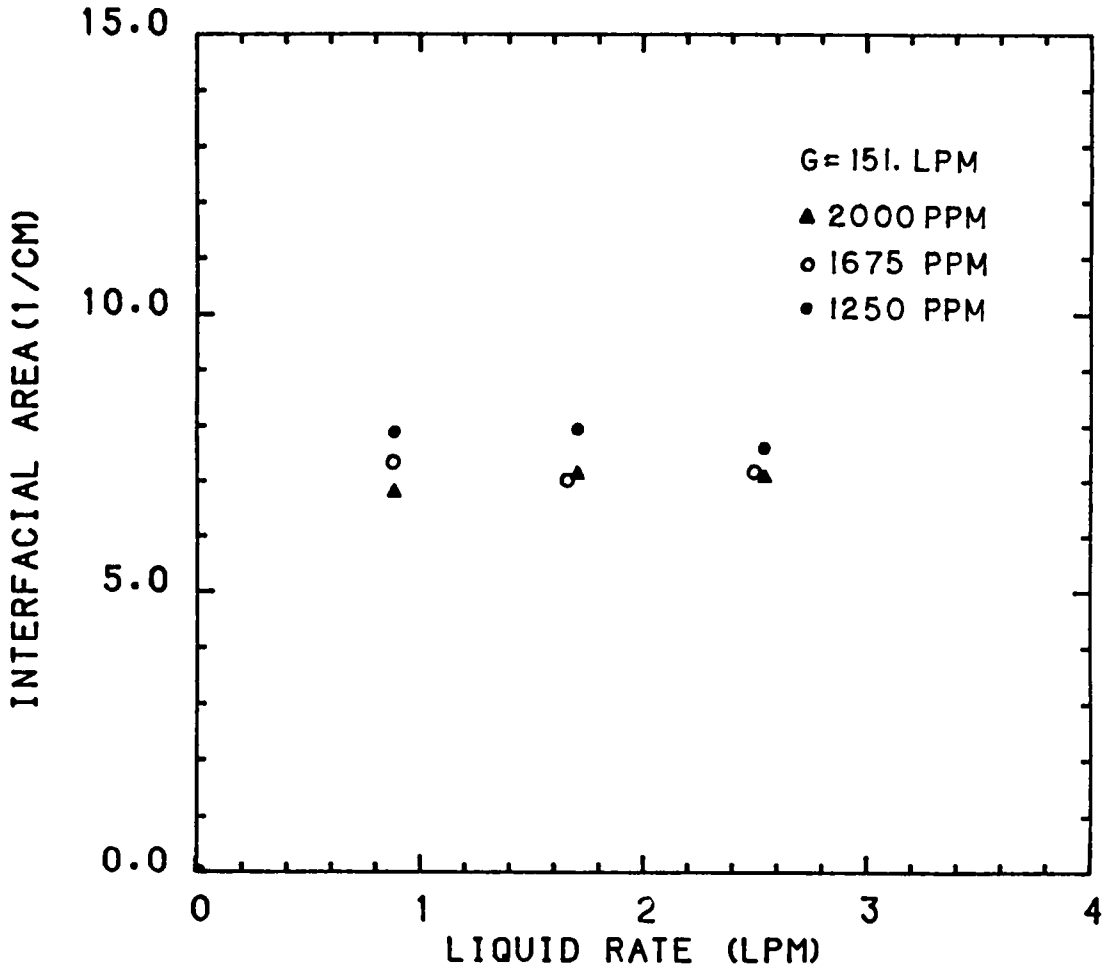

5-10. Interfacial area versus liquid rate at various inlet NO_2^* concentrations--gas rate is 151.0 LPM.

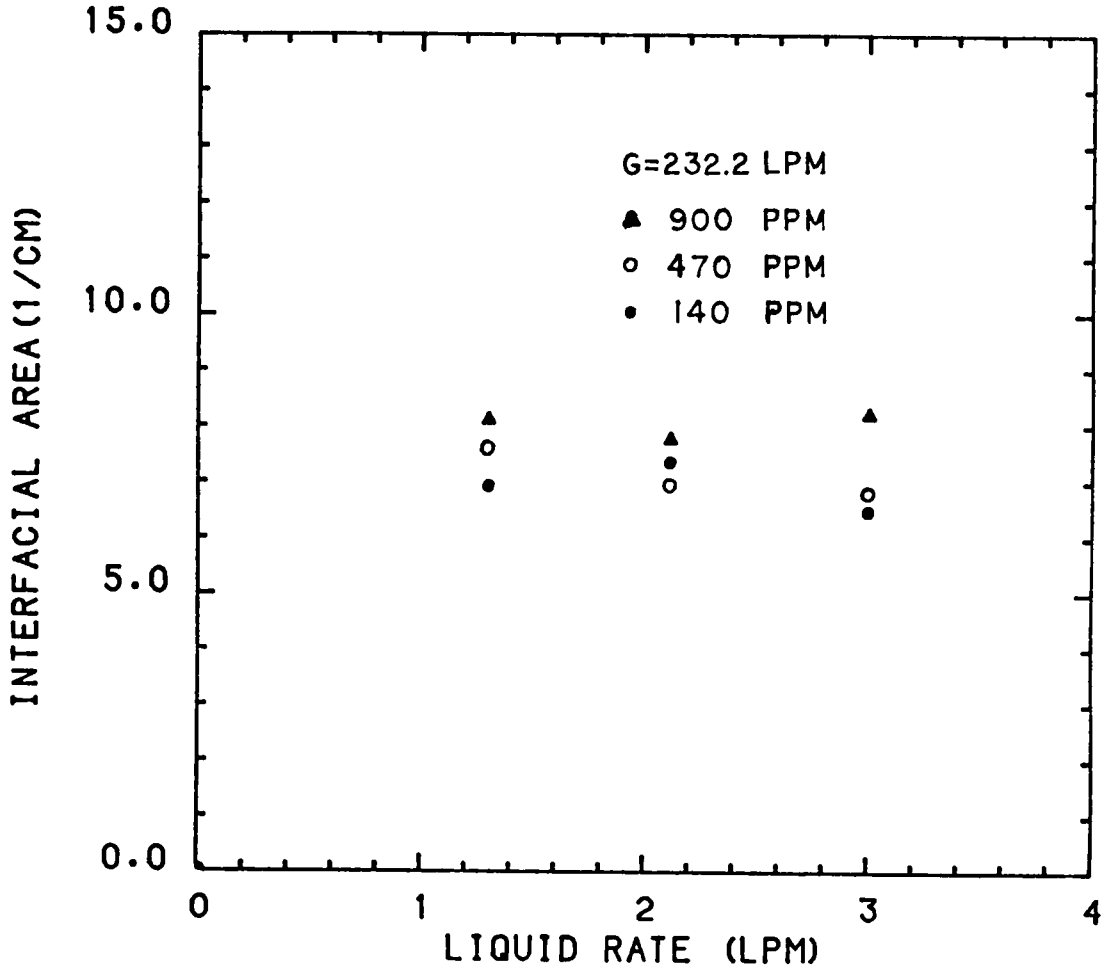

5-11. Interfacial area versus liquid rate at various inlet NO_2^* concentrations--gas rate is 232.2 LPM.

Figures 5-12 through 5-15 show the interfacial area versus gas rate. The other variables are liquid rate and inlet NO_2^* partial pressure. These figures show that interfacial area increases with increasing gas rate. This probably indicates the presence of some gas-phase resistance.

Figure 5-16 shows the interfacial area versus the inlet NO_2^* partial pressures at various gas rates. Liquid rate is not shown here because of the results of Figures 5-9 through 5-11. Over the concentration range studied, the interfacial areas, as calculated from the proposed model, appear to remain fairly constant. The average interfacial area (690. m^{-1}) is also shown.

Figure 5-17 shows the inlet and outline NO_2^* partial pressures for each experimental run. Also shown are lines representing the model equation at each gas rate. The model appears to describe the experimental data better at the higher gas rates. This would seem likely since gas-phase resistance, a term not present in the model equation, would be more prevalent at the lower gas rates.

If pure NO_2 were absorbed into water, the gas-phase resistance could be eliminated. Therefore some gas-phase resistance should be present, as evidenced by Figures 5-12 through 5-15 and by Figure 5-17. It is

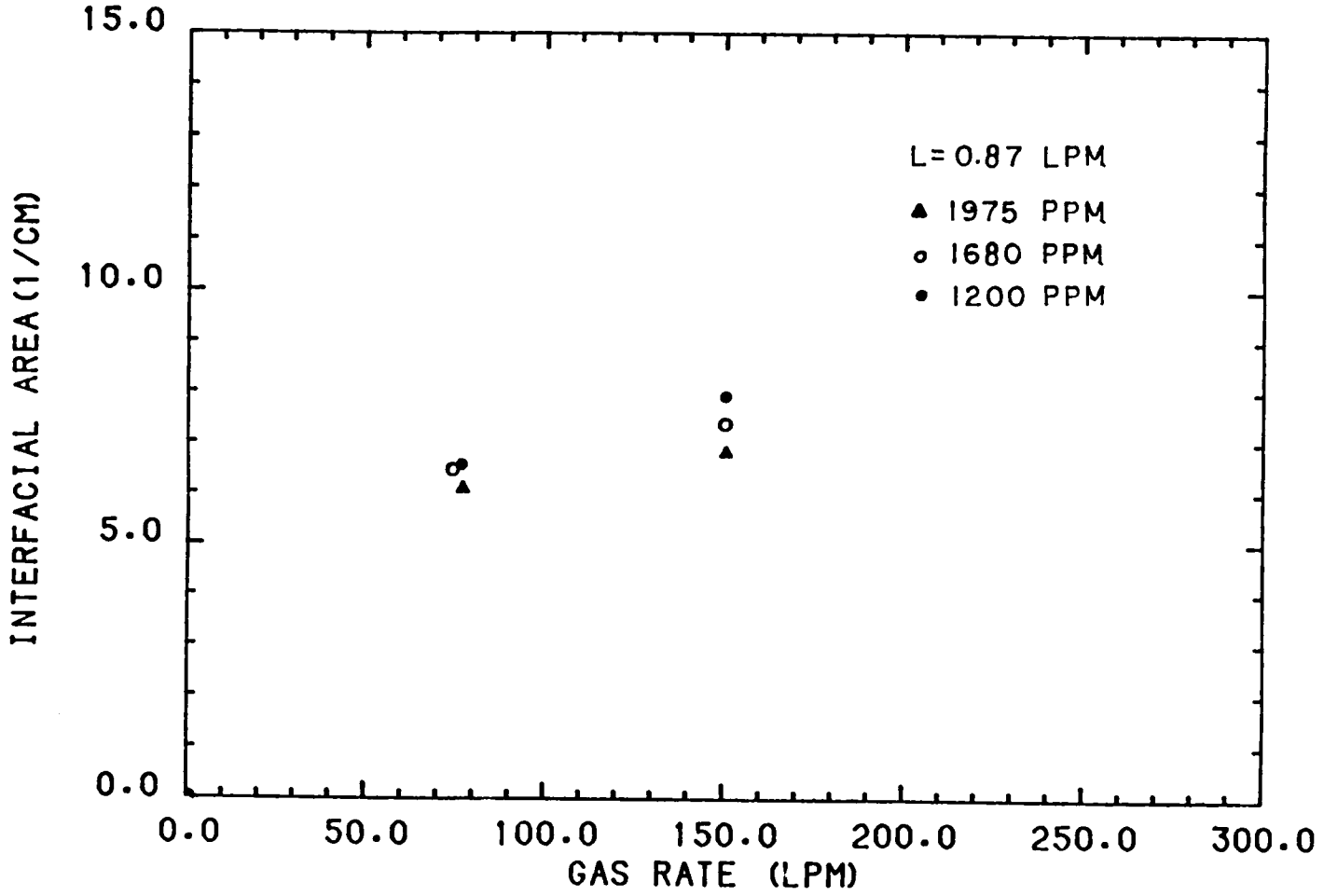

5-12. Interfacial area versus gas rate at various inlet NO_2^* concentrations--liquid rate is 0.87 LPM.

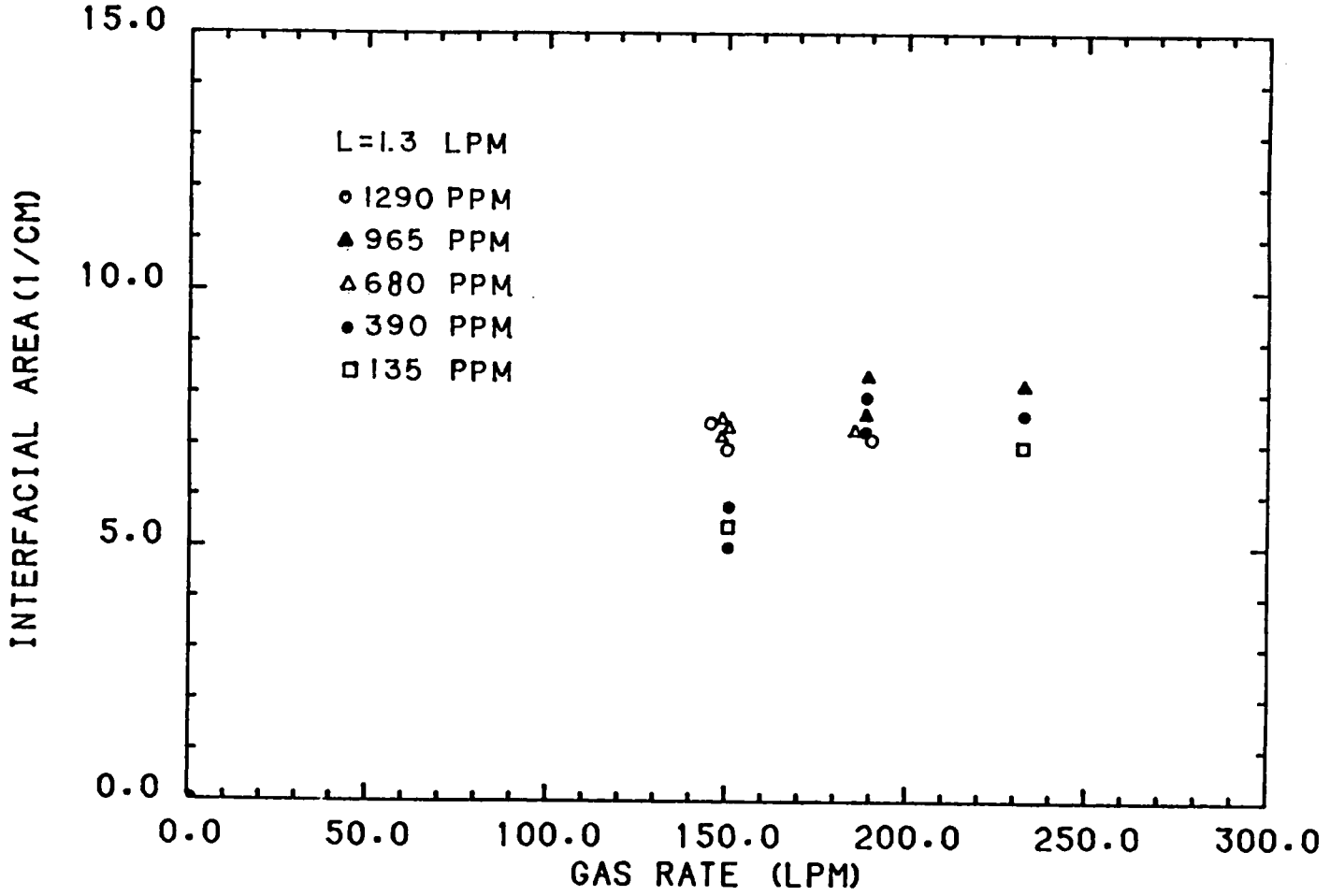

5-13. Interfacial area versus gas rate at various inlet NO_2^* concentrations--liquid rate is 1.3 LPM.

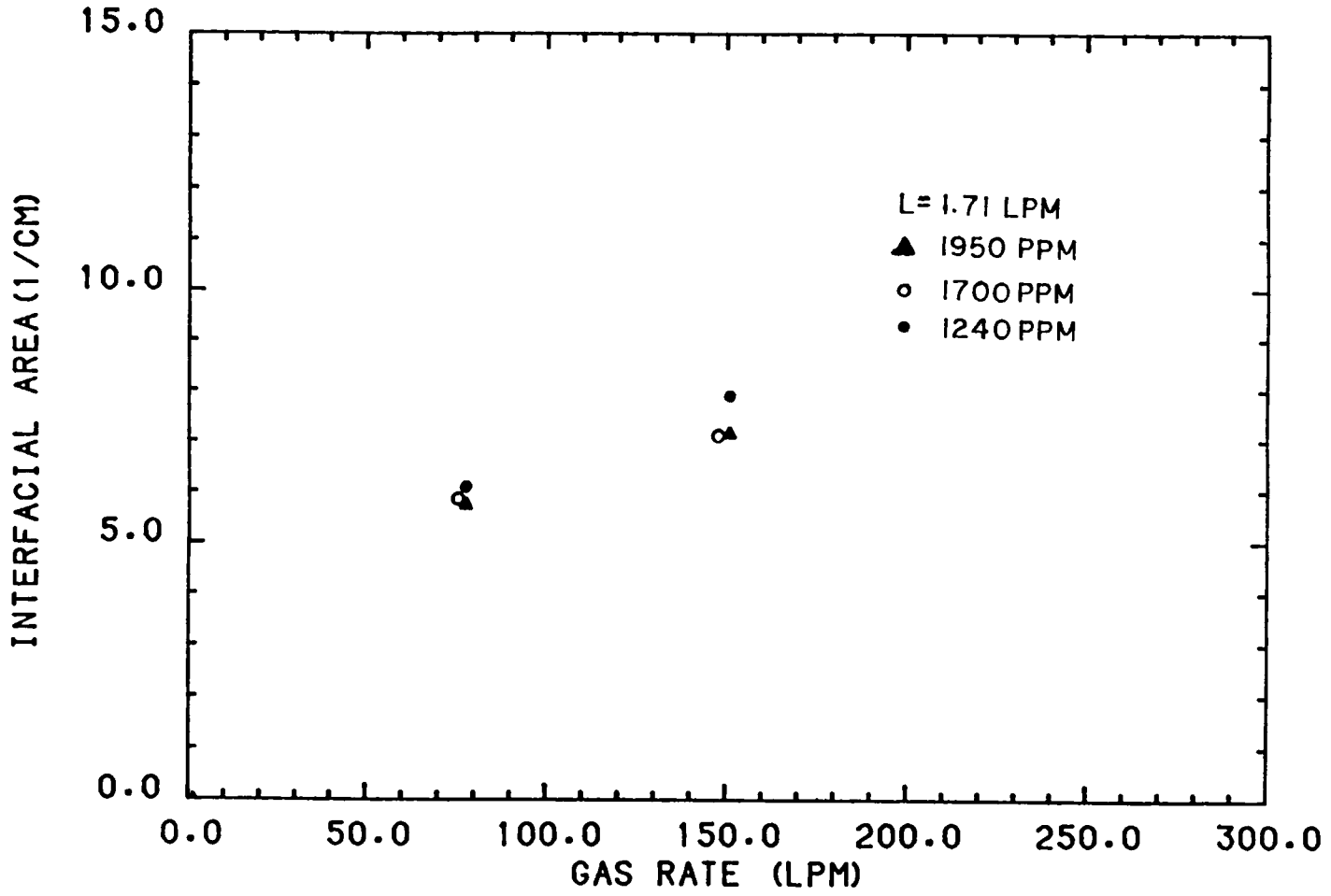

5-14. Interfacial area versus gas rate at various inlet NO_2^* concentrations--liquid rate is 1.71 LPM.

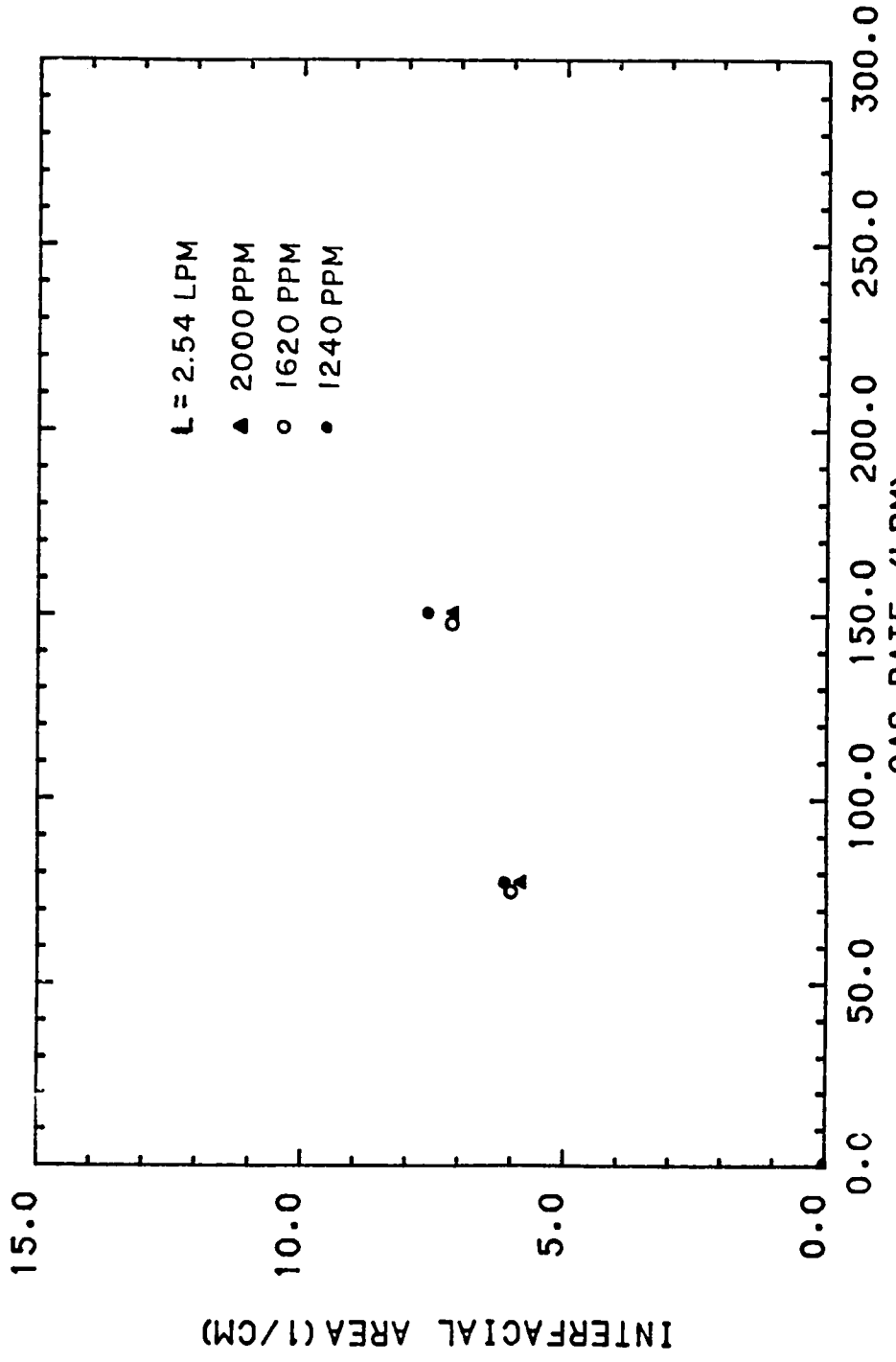

5-15. Interfacial area versus gas rate at various inlet NO_2^* concentrations--liquid rate is 2.54 LPM.

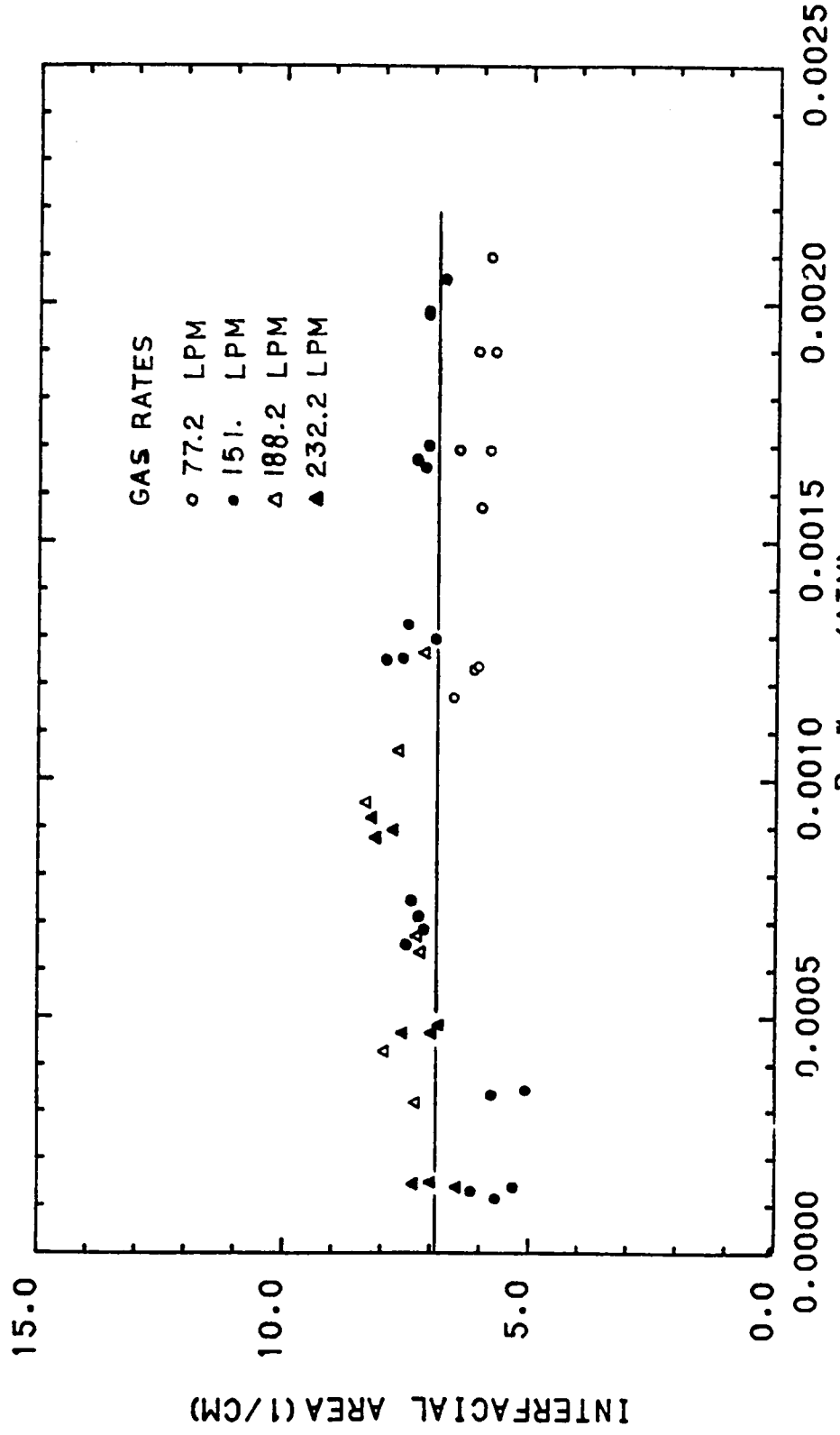

5-16. Interfacial area versus inlet NO_2^* concentration at various gas rates.

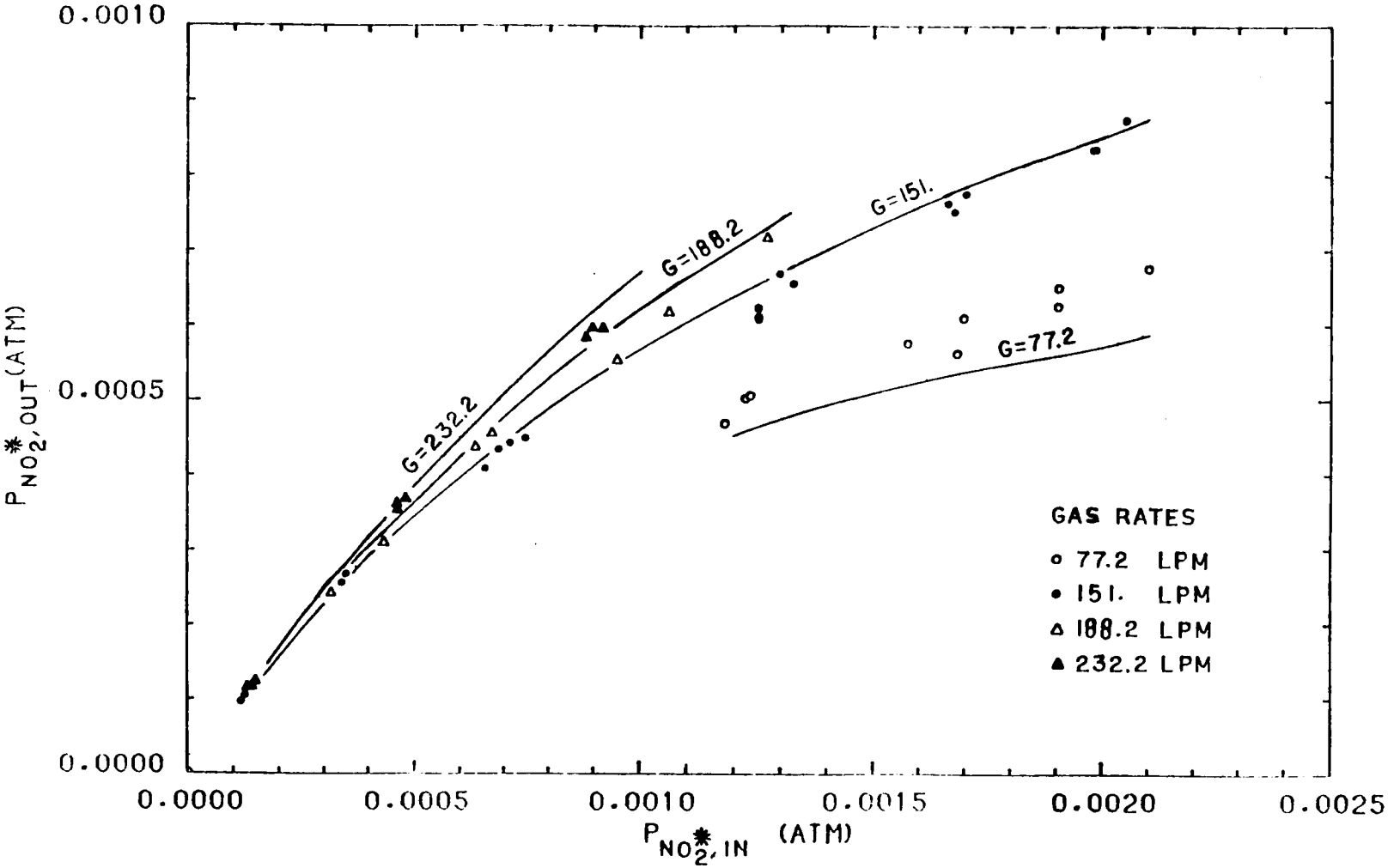

5-17. Inlet NO_2^* concentration versus outlet NO_2^* concentration at various gas rates.

recommended that the average interfacial area of 690. m^{-1} be treated as a conservative estimate in future studies.

The value of k_L appears to be in the reasonable range of mass-transfer coefficients. In general, good material balances were not obtained. At the higher NO_2^* concentrations the nitric and nitrous acid species could be detected in the outlet water samples. As the NO_2^* concentration was lowered, these acid species became less evident and eventually almost undetectable.

CHAPTER 6

CONCLUSIONS AND RECOMMENDATIONS

Conclusions

1. The model equation based on the absorption/hydrolysis of N_2O_4 and the absorption of NO_2 describes the pilot-plant scale NO_x scrubbing data well for the conditions studied.
2. At the concentration levels studied, the important absorbing species appear to be NO_2 and N_2O_4.
3. An interfacial area of 690. m^{-1} has been calculated from analysis of the data. It appears to remain fairly constant with varying liquid rate, which is in agreement with other publications.
4. A value of 4.982×10^{-4} m/s has been determined for the liquid-phase mass transfer coefficient. This value is reasonable compared to k_L values for other types of packing material.

Recommendations

1. Experimental work should be conducted where significant amounts of NO are present, preferably using a structured packing. This would help in understanding the importance of N_2O_3 absorption for this system.

2. The effects of temperature and pressure on this system should be studied in order to aid in the design of future NO_x absorption processes.
3. The average interfacial area calculated from this work should be treated as a conservative estimate for future studies.

LIST OF REFERENCES

LIST OF REFERENCES

Abel, E., and E. Neusser, Monatsh. Chem. 54: 855 (1929).

Andrews, S. P., and D. Hanson, Chem. Eng. Sci. 14: 105 (1961).

Ashmore, P. G., and B. J. Tyler, J. Chem. Soc. 1017 (1961).

Beattie, I. R., and S. M. Bell, J. Chem. Soc. 1681 (1957).

Bodenstein, M., Z. Elektrochem. 100: 68 (1918).

Bomio, P., Sulzer Technical Review 2, 62 (1979).

Bronsted, J. N., Z. Phys. Chem. 102: 169 (1922).

Corriveau, C. E., Jr., The Absorption of N_2O_4 into Water, Master's Thesis in Chemical Engineering, University of California, Berkeley (1971).

Counce, R. M., The Scrubbing of Gaseous Nitrogen Oxides in Packed Towers, Master's Thesis, University of Tennessee, Knoxville (1978).

Danckwerts, P. V., Gas Liquid Reactions, McGraw-Hill, New York, (1970), 146.

England, C., and W. H. Corcoran, Ind. Eng. Chem. Fundam. 13: 373 (1974).

Forsythe, W. R., and W. F. Giauque, J. Am. Chem. Soc. 64: 48 (1942).

Goyer, G. G., J. of Colloid Sci. 18: 616 (1963).

Greig, J. D., and P. G. Hall, Trans. Faraday Soc. 63: 655 (1967).

Hasche, R. L., and W. A. Patrick, J. Am. Chem. Soc. 46: 1207 (1925).

Hoftyzer, P. J., and F. J. G. Kwanten, Processes for Air Pollution Control, 2nd. ed., Chemical Rubber Co., Cleveland, 1972, Chap. 5B.

Kameoka, Y., and R. L. Pigford, Ind. Eng. Chem. Fundam. 16: 163 (1977).

Karavaev, M. M., and G. A. Skvortsov, Russ. J. Phys. Chem. 36 (5): 566 (1962).

Komiyama, H., and H. Inoue, 6th International Symposium on Chemical Reaction Engineering, Nice, France, D 20 (1980).

Kramers, H., M. P. P. Blind, and E. Snoeck, Chem. Eng. Sci. 14: 115 (1961).

Lee, Y. N., and S. E. Schwartz, J. Phys. Chem. 85: 840 (1981).

Lefers, J. B., F. C. De Boko, C. M. Van den Bleek, and P. J. Van den Berg, 6th International Symposium on Chemical Reaction Engineering, Nice, France, D 20 (1980).

Loomis, A. L., International Critical Tables III: 255, McGraw-Hill, New York (1928).

McKinnon, I. R., J. G. Mathieson, and I. R. Wilson, J. Phys. Chem. 83: 7 (1979).

Morrison, M. E., R. C. Rinker, and W. H. Corcoran, Ind. Eng. Chem. Fundam. 5: 175 (1966).

Sherwood, T. K., R. L. Pigford, and C. R. Wilke, Mass Transfer, McGraw-Hill, New York, (1975), Chap. 8.

Smith, J. H., J. Am. Chem. Soc. 69: 1742 (1947).

Treacy, J. C., and F. Daniels, J. Am. Chem. Soc. 77: 2033 (1955).

Verhoek, F. H., and F. J. Daniels, J. Am. Chem. Soc. 53: 1250 (1931).

Waldorf, D. M., and A. L. Babb, J. Chem. Phys. 40: 1165 (1964), 39: 432 (1963).

Wayne, L. G., and D. M. Yost, J. Chem. Phys. 19: 41 (1951).

Wendell, W. M., and R. L. Pigford, AICHE J. 4: 249 (1958).

APPENDICES

APPENDIX A

Table A-1. Experimental Data Readings.

Run	Temp. (°C)	Liquid Rate (LPM)	Gas Rate (LPM)	In		Out		pH,in	pH,out
				NO_x	NO	NO_x	NO		
1	22.0	1.3	232.2	150	5	130	5	8.37	8.15
2	22.0	2.12	232.2	145	5	125	5	7.55	7.4
3	22.0	3.0	232.2	145	10	125	7	7.35	7.25
4	22.0	1.3	232.2	520	55	405	50	7.3	6.93
5	22.0	2.12	232.2	530	65	415	53	7.2	7.13
6	22.0	3.0	232.2	540	65	425	55	7.17	7.15
7	22.0	1.3	232.2	1025	140	695	115	7.2	3.93
8	22.0	2.12	232.2	1040	145	705	110	6.85	6.45
9	22.0	3.0	232.2	1075	155	715	120	7.6	7.17
10	22.5	1.3	151.0	130	0	110	0	7.9	7.9
11	22.5	1.3	151.0	127	0	105	0	7.6	7.75
12	22.5	1.3	151.0	115	0	97	0	7.13	7.1
13	22.5	1.3	151.0	780	125	490	80	7.25	6.0
14	22.5	1.3	151.0	800	120	510	80	7.2	4.8
15	22.5	1.3	151.0	840	130	520	80	7.17	4.55
16	22.5	1.3	151.0	880	140	540	90	7.1	4.4
17	22.5	1.3	151.0	1625	300	865	210	7.5	3.4
18	22.5	1.3	151.0	1575	280	885	215	6.95	3.3
19	22.5	1.3	151.0	385	45	305	35	6.9	6.83
20	22.5	1.3	151.0	375	45	290	35	7.65	7.55
21	22.0	1.3	188.2	330	17	255	13	7.2	7.2
22	22.0	1.3	188.2	480	50	355	45	7.2	7.07
23	22.0	1.3	188.2	735	105	510	75	7.15	6.45
24	22.0	1.3	188.2	1525	260	945	225	7.15	3.2
25	22.0	1.3	188.2	1275	215	800	180	7.25	3.43

Table A-1 (Continued)

Run	Temp. (°C)	Liquid Rate (LPM)	Gas Rate (LPM)	In		Out		$pH_{,in}$	$pH_{,out}$
				NO_x	NO	NO_x	NO		
26	22.0	1.3	188.2	1150	200	730	175	7.17	3.45
27	22.0	1.3	188.2	820	150	565	110	7.2	6.15
28	22.5	0.87	151.0	1488	237	825	212	7.7	3.07
29	22.5	1.71	151.0	1500	250	819	209	7.0	3.6
30	22.5	2.54	151.0	1500	250	838	212	7.0	4.05
31	22.5	0.87	151.0	2037	363	1063	308	7.0	2.83
32	22.5	1.71	151.0	2050	250	1075	300	6.95	3.23
33	22.5	2.54	151.0	2037	275	1075	313	6.9	3.5
34	22.5	0.87	151.0	2500	450	1263	387	6.9	2.67
35	22.5	1.71	151.0	2450	465	1213	377	6.9	3.05
36	22.5	2.54	151.0	2450	475	1213	377	6.9	3.33
37	25.0	0.87	77.2	1438	263	638	169	7.65	3.33
38	25.0	1.71	77.2	1512	281	675	169	6.95	3.9
39	25.0	2.54	77.2	1537	312	688	187	7.15	5.0
40	25.0	0.87	77.2	2125	444	863	300	6.95	2.95
41	25.0	1.71	77.2	2125	431	900	288	7.0	3.45
42	25.0	2.54	77.2	2000	431	875	300	7.15	3.95
43	25.0	0.87	77.2	2450	550	1000	378	6.9	2.85
44	25.0	1.71	77.2	2475	575	1025	375	7.0	3.27
45	25.0	2.54	77.2	2700	600	1112	438	7.0	3.4

APPENDIX B

Verification of the Assumption that $\frac{ppm}{10^6} \cong$ Partial Pressure

The basis for this assumption will be 10^{-3} m^3 of air which has a concentration of 2000 ppm (a high concentration for this work) of pollutant. Temperature will be 298 K and total pressure will be 1 atmosphere. All gases are assumed to behave ideally. From the definition of ppm the volume of pollutant can be found:

$$ppm = \left(\frac{\text{Volume of Pollutant}}{\text{Volume of Air}}\right) \times 10^6$$

$$2000 \text{ ppm} = \left(\frac{\text{Volume of Pollutant}}{10^{-3} \text{ m}^3}\right) \times 10^6$$

$$\text{Volume of Pollutant} = 2 \times 10^{-6} \text{ m}^3$$

From the ideal gas law the number of moles of each gas can be calculated. Air is assumed to be one gas:

$$PV = n_i RT$$

$$1 \text{ atm } (10^{-3} \text{ m}^3) = n_{air}\left(0.08205 \frac{\text{m}^3 - \text{atm}}{\text{kgmol} - \text{K}}\right) (298 \text{ K})$$

$$N_{air} = 4.0898 \times 10^{-5} \text{ kgmol}$$

$$1 \text{ atm } (2 \times 10^{-6} \text{ m}^3) = n_{poll} \left(0108205 \frac{\text{m}^3 - \text{atm}}{\text{kgmol} - \text{K}} \right)^{68}_{(298 \text{ K})}$$

$$n_{poll} = 8.1797 \times 10^{-8} \text{ kgmol}$$

$$n_{total} = n_{air} + n_{poll} = 4.098 \times 10^{-5} \text{ kgmol}$$

The mole fraction of pollutant is,

$$Y_{poll} = \frac{n_{poll}}{n_{total}} = 0.001996$$

Since the total pressure is 1 atmosphere, the mole fraction is equal to the partial pressure,

$$P_{poll} = Y_{poll} = 0.001996$$

The percent error is calculated as,

$$\% \text{ error} = \left(\frac{\frac{2000}{10^6} - 0.001996}{\frac{2000}{10^6}} \right) \times 100$$

$$\% \text{ error} = 0.2$$

APPENDIX C

Procedure to Calculate Gas-Phase Partial Pressures

The partial pressure of NO_2^* can be approximated by subtracting the NO ppm reading from the NO_x ppm reading and dividing by 10^6:

$$P_{NO_2}^* = P_{NO_2} + 2P_{N_2O_4} \cong \frac{NO_x(ppm) - NO(ppm)}{10^6} \qquad (C\text{-}1)$$

The equilbirium constant K_1 can be defined as,

$$K_1 = \frac{(1-\alpha^2)}{4\alpha^2}\left(\frac{P_T}{P_{NO_2}+P_{N_2O_4}}\right) \qquad (C\text{-}2)$$

where α is the fraction of the N_2O_4 which is dissociated.

The ratio of NO_2 to N_2O_4 in the gas phase is,

$$\frac{P_{NO_2}}{P_{N_2O_4}} = \frac{2\alpha}{1-\alpha} \qquad (C\text{-}3)$$

K_1 is determined by the system temperature and the $P_{NO_2}^*$ is known from the NO_x and NO readings. There are three equations (C-1, C-2, and C-3) and three unknowns (α, P_{NO_2}, $P_{N_2O_4}$). Substituting (C-3) into (C-1) and (C-2) gives,

$$P_{NO_2}^{*} = \frac{2P_{N_2O_4}}{1-\alpha} \qquad \text{(C-4)}$$

$$K_1 = \frac{(1-\alpha)^2}{P_{N_2O_4}(4\alpha^2)} \qquad \text{(C-5)}$$

Eliminating $P_{N_2O_4}$ from equations (C-4) and (C-5) allows the calculation of α from the system temperature and the NO_x/NO readings. The partial pressures of N_2O_4 and NO_2 can then be calculated from equations (C-5) and (C-3) respectively.

APPENDIX D

Derivation of First Model

The derivation of the first model begins with a flux equation,

$$-G'(dY_{NO_2}^*) = N_{NO_2}^* a_i (dz) \qquad \text{(D-1)}$$

In addition to the second models assumptions, this model assumes that N_2O_4 is the only absorbing specie. The flux of NO_2^* is defined as,

$$N_{NO_2}^* = 2\left(\frac{\sqrt{Dk_7}}{H}\right)_{N_2O_4} P_{N_2O_4} \qquad \text{(D-2)}$$

Also the equilibrium relationship between NO_2 and N_2O_4 is,

$$P_{N_2O_4} = K_1 (P_{NO_2})^2 \qquad \text{(3-4)}$$

Combining equations (D-1), (D-2), and (3-4) and assuming that $P_{NO_2} \cong Y_{NO_2}^*(P_T)$ gives,

$$-G'(dY_{NO_2}^*) = 2\left(\frac{\sqrt{Dk_7}}{H}\right)_{N_2O_4} K_1 P_T^2 (Y_{NO_2}^*)^2 a_i (dz) \qquad \text{(D-3)}$$

Separating and integrating gives the final form of the models equation,

$$-\int_{in}^{out} \frac{dY_{NO_2}^*}{(Y_{NO_2}^*)^2} = \frac{2\left(\frac{\sqrt{Dk_7}}{H}\right)_{N_2O_4} K_1 P_T^2 a_i}{G'} \int dz \qquad (D\text{-}4)$$

$$(Y_{NO_2}^*,out)^{-1} - (Y_{NO_2}^*,in)^{-1} = \frac{2\left(\frac{\sqrt{Dk_7}}{H}\right)_{N_2O_4} K_1 P_T^2 a_i Z}{G'} \qquad (D\text{-}5)$$

VITA

Gary W. Selby was born in Rockwood, Tennessee, on March 9, 1960 and was reared in Kingston, Tennessee. He was graduated from Roane County High School in June 1978. In August 1982 he received his Bachelor of Science degree in Chemical Engineering from Tennessee Technological University. He began his graduate studies in March 1984 at The University of Tennessee, Knoxville, and received the Master of Science degree with a major in Chemical Engineering in June 1986.